Technical University of Denmark

DTU

Simulation of shear and turbulence impact on wind turbine performance

Wagner, Rozenn; Courtney, Michael; Larsen, Torben J.; Schmidt Paulsen, Uwe

DTU Library
Technical Information Center of Denmark

Simulation of shear and turbulence impact on wind turbine performance

Author: Wagner Rozenn, Courtney S. Michael, Larsen J. Torben, Paulsen S. Uwe
Title: Simulation of shear and turbulence impact on wind turbine power performance
Division: Wind Energy

Abstract:
Aerodynamic simulations (HAWC2Aero) were used to investigate the influence of the speed shear, the direction shear and the turbulence intensity on the power output of a multi-megawatt turbine. First simulation cases with laminar flow and power law wind speed profiles were compared to the case of a uniform inflow. Secondly, a similar analysis was done for cases with direction shear. In each case, we derived a standard power curve (function of the wind speed at hub height) and power curves obtained with various definitions of equivalent wind speed in order to reduce the scatter due to shear. Thirdly, the variations of the power output and the power curve were analysed for various turbulence intensities. Furthermore, the equivalent speed method was successfully tested on a power curve resulting from simulations cases combining shear and turbulence. Finally, we roughly simulated the wind speed measurements we may get from a LIDAR mounted on the nacelle of the turbine (measuring upwind) and we investigated different ways of deriving an equivalent wind speed from such measurements.

Contents

Preface

This work was performed as a task under the IMPER project.

1 Introduction

The power output of a given wind turbine primarily depends on the mean speed of the inflow. The aerodynamic behavior of a horizontal axis wind turbine in a uniform inflow, i.e. same wind speed magnitude and direction at all points, is today well understood and can be modeled quite accurately. However, the inflow is usually non uniform because of the wind shear, i.e. variations in the wind speed and direction profiles, and turbulence, i.e. fast fluctuations of the wind speed and directions around the mean profiles, or the aerodynamics is influenced by skew wind originating from misalignment between the rotor axis and the wind direction. The IEC standard for power curve measurement (61400-12-1) requires presently only the measurement of wind speed at hub height within a wind direction sector. Surveys and fact findings on the causes and consequences of flow variability and turbulence on horizontal wind turbines have been carried out in the 80'ties (Christensen, 1988), and (Elliott, 1990) showed that wind speed profiles had an influence on the wind turbine power curve. Interest for this influence has recently been motivated (Sumner, 2006; Albers, 2007; Wagner, 2008; Antoniou, 2009; Walter, 2009) as the size of wind turbines has been considerably growing over the last decade, implying a higher hub height (at least 80m) and a larger rotor (more than 100m of diameter) that is inclined to experience larger variations of speed and direction.

The influence of non uniform flow on the power output from a horizontal axis wind turbine is complicated since each section of the rotor blade is subjected to spatial and temporally varying wind during rotation. Investigating the effects on the turbine power output of shear and turbulence is not straightforward since these parameters are correlated. For example, a stable stratified surface layer generally implies low turbulence and high shear. At the other extreme, in an unstable boundary layer, the speed profile is generally nearly constant because of the thermal mixing (Van den Berg, 2008; Swawell, 2008). Because of this correlation, it is difficult to investigate the influence on the power output of shear independently of turbulence.

Numerical models of wind turbine aerodynamics are broadly used and constantly developed in order to investigate the loads on the turbine structure. Such models enable us to investigate the effect of various parameters independently of each other which, due to the close correlation between parameters, can be difficult or impossible from analyzing real data. This is why, in the work presented here, we used an aerodynamic model to investigate the influence of various wind parameters on the power output of a multi-megawatt wind turbine. Simplified cases were simulated with an aerodynamic model similarly to the work presented in (Walter, 2007).

The model we used was HAWC2Aero, which is a simplified version of the aeroelastic code developed at Risø DTU: HAWC2. The turbine modeled was a 3.6 MW Siemens, with a rotor diameter of 107m, hub height of 90 m and a variable-speed, variable-(collective) pitch control strategy. The rotation speed was limited to a maximum of 1.963 rad/s for noise reduction. Once this maximum is reached for a given wind speed (here about 5m/s), the rotation speed remains constant for higher wind speeds.

This investigation focuses on the effect of the vertical shear, i.e. vertical variation of the horizontal wind speed and direction. However, in order to be able to relate the results to experimental data, the influence of turbulence was also investigated.

The overall aim of this work is to relate the variation in power curve scatter to the wind conditions encountered by the turbine. In order to restrict the variations in power to the variations due to the wind conditions (and not to any other effect), each case is assumed as simple as possible. Thus horizontal homogeneity of the lower part of the boundary layer (corresponding to the "turbine layer" where the turbine rotor stands) is assumed in the whole investigation. This means that the wind speed and direction can vary vertically, but

they are assumed over flat terrain to be independent and uniform in horizontal planes at each height: $\langle u(x,y,z) \rangle = \langle u(z) \rangle = \langle (u_x(z), u_y(z), u_z(z)) \rangle$.

The next section provides a description of the model used, with an emphasis on its limitations. The following sections present the simulated effects of the wind speed shear (section 3), of the direction shear (section 4) and of the turbulence intensity (section 5). In section 6 results are shown for more realistic inflow mixing shear and turbulence. These four sections are all based on the assumption that the wind speed is given at different heights along the vertical axis in the middle of the swept rotor area (however since horizontal homogeneity is assumed this does not matter). Section 7 presents another configuration where the wind speed is given around a circle within the swept rotor area. The idea is to get a first approach of what could be obtained with a LIDAR mounted on the nacelle of the turbine and measuring forward.

As a partner of the IMPER project, Vestas carried out similar simulations with their own model for a V90 turbine. The results from those simulations are presented in section 6 and 7.

2 Aerodynamic model

Aerodynamics

The aerodynamics of the turbine was simulated using the computer code HAWC2Aero. This numerical model simulates in the time domain, the response of a rigid rotor subjected to aerodynamic forces. The code is a simplified version of the full aeroelastic code HAWC2 with a different (rigid) structural model.

HAWC2 is intended for calculating wind turbine response in the time domain and has a structural formulation based on multi-body dynamics. The aerodynamic part of the code is based on the blade element momentum (BEM) theory, but extended from the classic approach to handle dynamic inflow, dynamic stall, skew inflow, shear effects on the induction and effects from large deflections (Larsen TJ, 2006; Larsen TJ 2006). Apart from a simplified structural formulation, all other substructures of the code in HAWC2 and HAWC2Aero are identical. In HAWC2Aero the rotor is assumed rigid which leaves only one degree of freedom namely the rotor rotation, whereas the HAWC2 code is based on a multibody formulation with very few limitations on the structural layout. The controller would change the pitch angle though, but only for wind speeds above rated power (which are not of interest in this study). The main benefit of the HAWC2Aero code is the simulation speed (app. 10 times faster than real time on a standard pc) and the reduced complexity of the input parameters compared to the full HAWC2 code.

In order to check if this simplification was acceptable, we run simulations with the full Hawc2 model (for a 5MW wind turbine) for both cases of elastic and stiff structures. For each type of structure, various wind speed at hub height were considered and for each wind speed two kinds of speed profiles: a uniform profile (same wind speed at all height) and a power law profile with a shear exponent of 0.5. It is the difference in power output obtained for those two kinds of profiles that is shown in Figure 2.1.
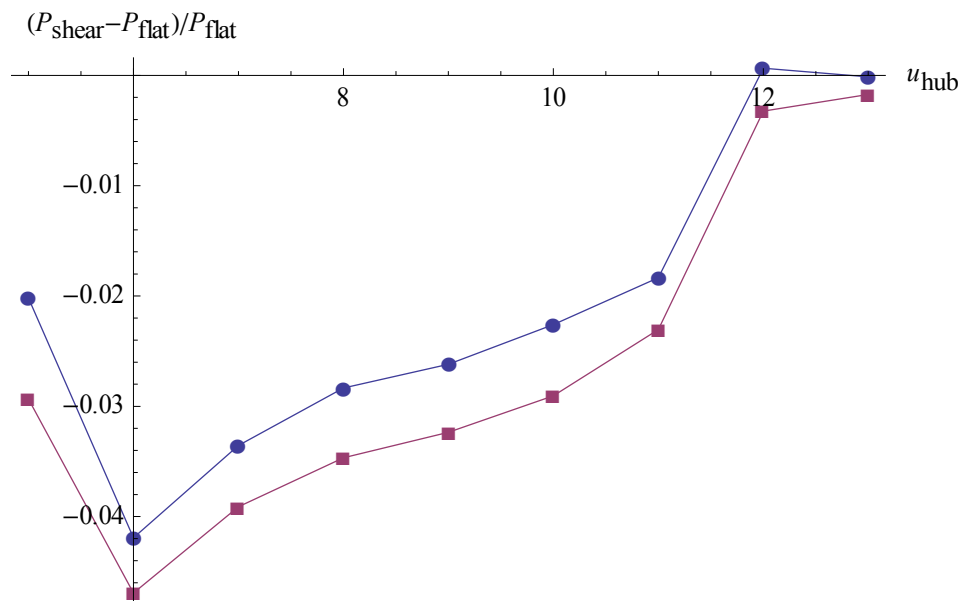
Figure 2.1 Blue: stiff structure; Red: Elastic structure. Simulations carried out with full Hawc2 model for a fictive 5MW wind turbine. Shear profile = power law with alpha=0.5.

The difference between the result obtained with the stiff structure and the elastic structure is small (in comparison to difference obtained between constant profile and shear). We consider that this shows typical results for multi-megawatt wind turbines. We therefore expect the same results with the turbine modeled in our investigation, thus this justifies the use of the simplified model in this report.

Wind shear and turbulence

HAWC2Aero offers the possibility to implement wind speed shear either with theoretical wind speed profiles such as power law profiles for example or with the user-defined-shear option that enables the user to describe a profile by giving the wind speed at various heights.

Superimposed on the mean wind speed profiles, the time variations of the three components of the wind speed are simulated by using the Mann model of turbulence. This is a spectral tensor model for the atmospheric surface layer turbulence under neutral stratification. The model assumes that the turbulence is homogeneous in space but non-isotropic and includes the influence of shear. The method generates a full three-dimensional turbulence field with all three components (Mann, 1994).

Limitations

The wind shear has a complex effect on the aerodynamics as the wind speed experience by each blade changes depending on its position. The consequences on the forces applied o the rotor and the resulting torque can be modeled in various ways. Therefore, different results can be obtained from one model to another. In the classic BEM method, the induction factor is assumed to be constant over the whole rotor disc, which is actually not true for a non uniform inflow. In the case of a vertical wind speed shear for example, the induced velocity is expected to be higher when the blade is upward (higher wind speed) than when the blade is downward. For this reason, the BEM method used in HAWC2 was modified so that the induced velocity varies with azimuth angle. The flow over the rotor is split in stream tubes (depending on the azimuth angle). In the stream tube, there is const. flow.

"The characteristic of this implementation of BEM with respect to wind shear is that the local thrust coefficient is based on the local loads of the blade at this specific point but normalized with the free stream velocity averaged over the whole rotor disc. The final induced velocity will thus vary along the blade as function of azimuth position of the blade." (Bak K., 2006; Risø-I-2522)

This code has been compared to a classic BEM code, Flex5, and two more advanced models, the Actuator Line model and the CFD based EllipSys3D code, in (Bak K., 2006). The wind shear was seen to cause different effect on the power output and a clear tendency of the shear on the power coefficient could not be extracted from those results. A conclusion of this investigation was that there is a high uncertainty regarding the influence of wind shear on the turbine rotor, probably because the induction was implemented in different ways in the various BEM models. Even the more advanced models did not demonstrate any convergence of the simulation results (see Table 1) that would allow any conclusions as to the correct method.

The power extraction model at the generator is not encountering un-linear interactions between the mechanical and electrical system, however as such the comparisons do not depend on this.

Another point though is that calculations might be sensitive on steepness of the Cp curve and the range where maximum Cp occurs around 6-8 m/s.

Table 1 Comparison of electrical power at 8 m/s for uniform inflow and shear inflow (power law with exponent of 0.5), from Risø-R-1611.

	El. power [kW] no shear	El. power [kW] shear
HAWC2	**1906**	**1812**
EllipSys3D	**1867**	**1830**
FLEX5	**1900**	**1932**
AC-Line	**1995**	**2135**

The results from the investigation presented here are therefore restricted to HAWC2Aero and the underlying modeling assumptions and uncertainties must be remembered. Despite the high uncertainty of the results, HAWC2Aero was a good compromise as it is based on an improved BEM model that, we believe, models the underlying physics in a convincing manner, yet has a low computational time. Moreover the tower shadow effect is turned off and the shaft tilt angle was set to 0°, in order to be able to observe the time/azimuth dependent variations of angle of attack and relative speed experienced by the blade due to the wind shear.

3 Effect of the wind speed shear

In this section, we focus on the effect of the wind speed vertical shear (i.e. variation of the horizontal wind speed with altitude) on the power output of the turbine. Note that for simplicity and as the aim of this investigation is to distinguish the effect of various wind characteristics, the results presented in this section were all obtained with laminar inflow (no turbulence). In doing so the flow is assumed to be layered stable in a continuous manner, without any effect from a layer to another one.

3.1 Simple aerodynamics considerations

In order to highlight the differences between a sheared inflow and a uniform inflow, various aerodynamic parameters were compared. For illustration, we consider a constant profile with a wind speed of 8 m/s ($u(z) = 8$ m/s) and a power law profile with wind speed of 8 m/s at hub height with an arbitrary power law exponent α=0.5 ($u(z) = 8\left(\dfrac{z}{z_{hub}}\right)^{\alpha}$)m/s. Both profiles are displayed in Figure 3.1.
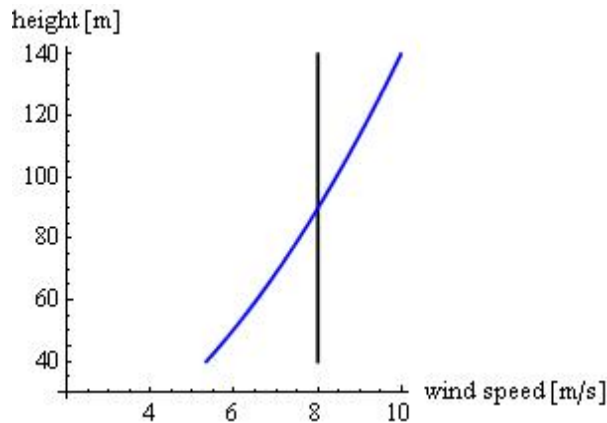
Figure 3. 1 Profiles used as input for the wind speed shear aerodynamic investigation. Black: no shear; Blue: power law profile with shear exponent of 0.5. Both profiles have the same wind speed at hub height.

Figure 3.2 shows the free wind speed $u_y(z, t)$ (i.e. the absolute wind speed as if there were no turbine) seen by a point at a radius of 30m from the rotor centre and rotating at the same speed as the rotor as a function of time. Whereas in a uniform flow the blade is subjected to a constant wind speed, in a sheared flow, the point is exposed to large variations of wind speed even though the inflow is laminar. The variation of the wind speed seen by this rotating point in time is only due to the fact that it is rotating within a non uniform flow (speed varying with altitude).

Figure 3. 2 Time series of free wind speed seen from a rotating point, positioned at a radius of 30m, rotating at rotor rotational speed (no induced velocity). Black: no shear; Blue: power law profile with shear exponent of 0.5.
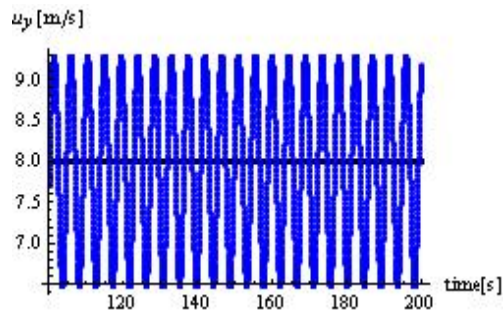
Figure 3.3 shows the variations of the free wind speed seen by the same rotating point as previously as function of the azimuth position (0 degrees = downwards). The point experiences the hub height wind speed when it is horizontal (+/- 90deg), lower wind speed when it is downward (0 deg) and higher wind speed when it is upward (180 deg). As the wind speed increases with height as in the case of the power law profile, the amplitude of the variations of the free wind speed seen by a rotating point increases with the radius (not shown here), whereas for a uniform flow, the free wind speed is the same whatever the position on the swept rotor disc (any radius, any azimuth).
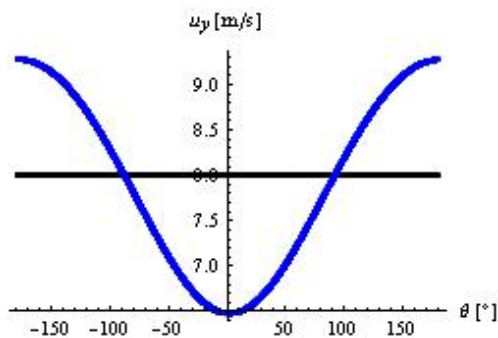
Figure 3. 3 Free wind speed seen from a rotating point, positioned at a radius of 30m, rotating at rotor rotational speed, as function of the azimuth angle. Black: no shear; Blue: power law profile with shear exponent of 0.5.

A rotating blade does not experience the free wind speed because of the induction due to the drag of the rotor. In reality, a rotating blade is directly subjected to the relative speed (i.e. the speed of the wind passing over the airfoil relative to the rotating blade.) and the angle of attack / i.e. the angle between the blade chord line and the relative wind speed) with the effects of the induced speed included. The variations of these two parameters as function of the azimuth angle are shown in Figure 3.4. As these two parameters directly depend on the free wind speed, they vary with the azimuth angle in a sheared inflow whereas they remain constant in a uniform inflow. We can see that the variation of the relative speed and the angle of attack present similar pattern to the free wind speed (see Figure 3.3).

Figure 3. 4 Angle of attack (left) and relative speed (including induction) (right) as a function of azimuth angle, seen from a point at radius r=30m on a rotating blade. Black: no shear; Blue: power law profile with shear exponent of 0.5.
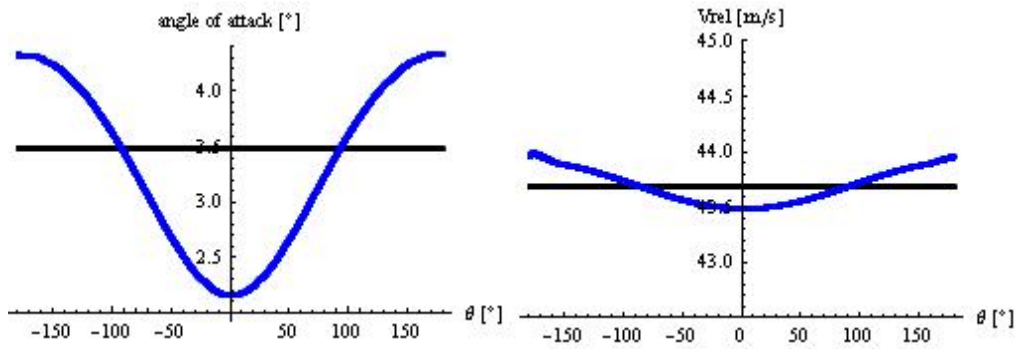
The relative speed and the angle of attack are derived from the rotor speed and the induced velocity, therefore they depend on the way the induction is modeled and it is difficult to evaluate their variations due to a non uniform flow in a simple way. However, some basic considerations (ignoring the induction) can give a basic insight to the variation of the relative speed and the angle of attack as the blade rotate, see Appendix A. When the blade looks upward, the free wind speed increases compared to the wind speed at hub height (or uniform inflow case), and so does the relative speed and the angle of attack. Inversely, when the blade looks downward, they decrease.

This causes a variation of the local lift and drag as the blade rotates, which finally results in the variation of the local tangential force, see Figure 3.5. The angle of attack (φ), the local lift (dF_L) and the local drag(dF_D) we obtained as output of the model and the local tangential force (dF_T) was calculated according to the BEM theory (Manwell et al. 2002):

$$dF_T = dF_L \sin(\varphi) - dF_D \cos(\varphi)$$

The variations in tangential force due to sheared inflow explain (at least partly) why in such a case the torque generated by the turbine is different from that obtained with a uniform inflow. As a consequence, sheared flows can affect the power output.
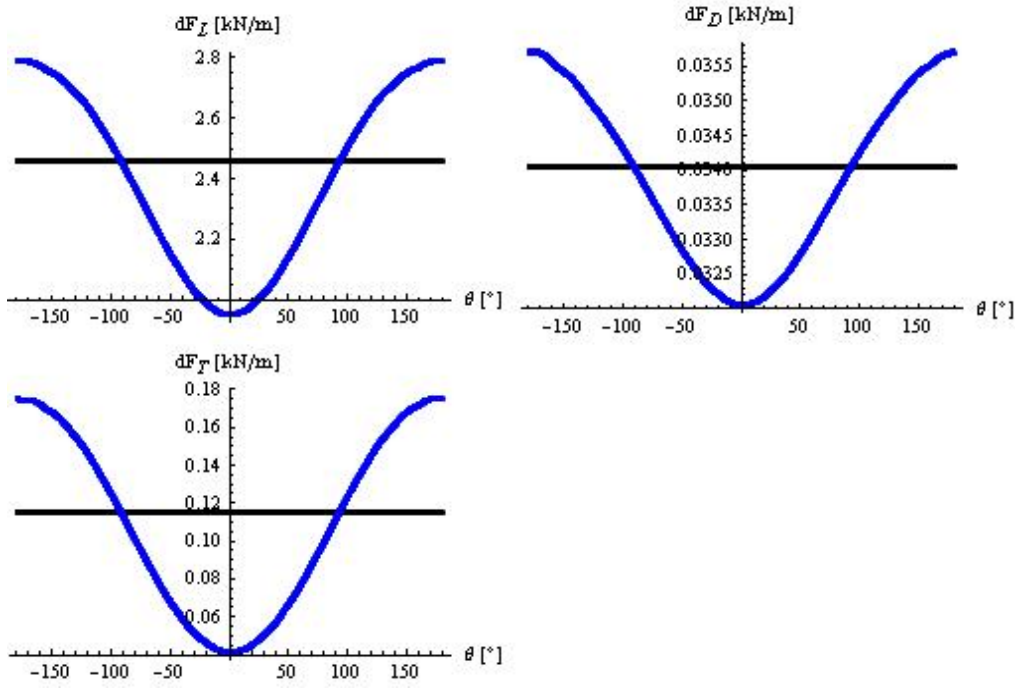
Figure 3. 5 Local lift (top left), local drag (top right), local tangential force (bottom) seen from a point at radius r=30m on a rotating blade as a function of its azimuth position. Blue: no shear; Red: power law profile with shear exponent of 0.5.

3.2 Consequences on the power production

In order to look at the effect of speed shear on the power output of the turbine, Figure 3.6 shows the difference between the power output obtained for a sheared profile, *P*, and the power output obtained with a uniform inflow for the same wind speed at hub height, $P_0^{u_{hub}}$, normalized by $P_0^{u_{hub}}$. The simulated cases were theoretical wind speed shear defined as a power law with a shear exponent between -0.1 and +0.5 ($u(z) = u_{hub}\left(\dfrac{z}{z_{hub}}\right)^{\alpha}$ m/s), for a range of wind speeds at hub height from 5 to 10 m/s.

The kinetic energy flux used to calculate the power coefficient (*Cp*) defined in the IEC standard 16400-12-1 takes only the wind speed at hub height into account (i.e. the wind speed is assumed constant with height):

$$KE_{hub} = \frac{1}{2}\rho u_{hub}^3 A$$

where *ρ* is the air density and *A* the rotor swept area.

A better approximation of the kinetic energy flux can obtained if the wind speed profile in front of the rotor swept area is taken into account (Wagner 2009):

$$KE_{profile} = \int_{H-R}^{H+R} \frac{1}{2}\rho u(z)^3 c(z - (H - R))dz$$

where H is the hub height, *c(z)* is the chord (of the circle defined by the rotor swept area) as function of the height z which varied between the bottom (lower tip
) and the top (higher tip) of the rotor::

$$c(z) = 2\sqrt{2Rz - z^2}$$

where *R* is the rotor radius.

In order to compare with the power output variations, Figure 3.6 shows the difference between the kinetic energy flux for power law profile and a constant profile normalised with the power obtained with a constant profile($(KE_{profile}-KE_{hub})/KE_{hub}$), see gray dashed line. (Note that the kinetic energy flux is not an output of HAWC2Aero, it has been calculated manually and for power law profiles, the normalized difference does not depend on the wind speed.)
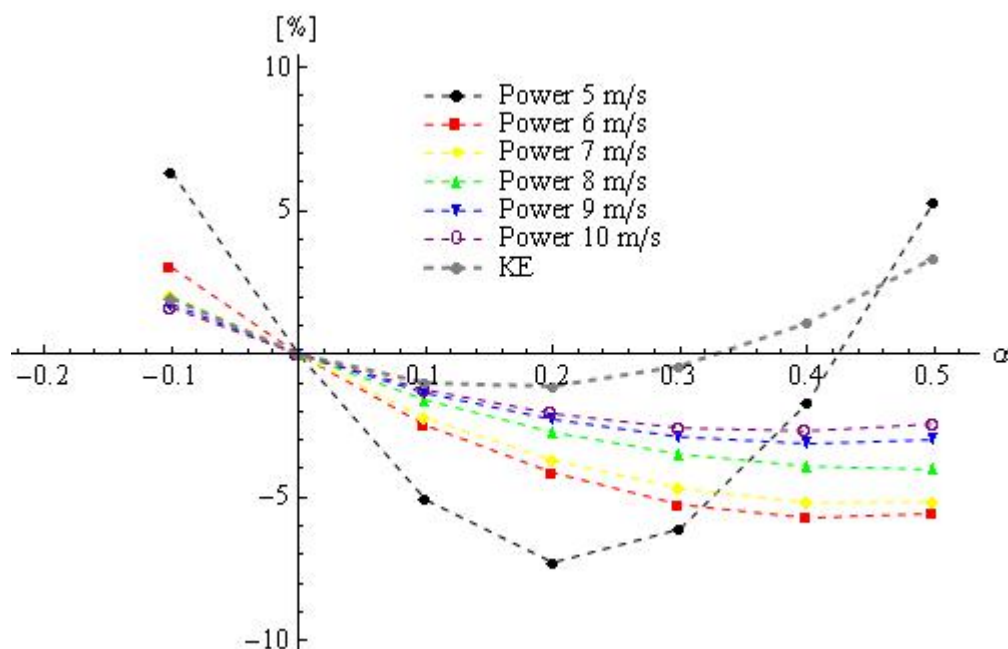

Figure 3. 6 Normalised difference in kinetic energy flux and in power output between shear case and uniform case as function of the shear exponent, for various wind speed at hub height.

Figure 3.6 shows two main results:
1) The kinetic energy flux varies with the shear exponent;
2) According to HAWC2Aero, the power output also depends on the shear exponent, for wind speeds above 5 m/s resulting in a decrease of the power with an increase of the shear exponent, and the power difference ($P - P_0^{u_{hub}}$) as function of shear exponent does not follow the same trend as the kinetic energy flux difference.

Despite the high uncertainty in the modeled power output for a sheared inflow, the results highlight that the influence of the shear on the power performance of a turbine can be seen as the combination of two effects:

-   the variation in kinetic energy flux (power input);
-   the ability of the turbine to extract the energy from the wind, which depends on the details of the design and the control strategy of the turbine.

Indeed if the turbine extracted the same amount of available kinetic energy for any shear exponent, we can think that the two graphs in figure 3.6 would follow a similar pattern. The fact that they are different shows that for high shear exponent (above 0.2 in this example) the turbine is not able to extract the same amount of energy as it does for a lower shear exponent.

3.3 Note on the relation between simulated power output and rotor averaged wind speed
We saw in 3.2 that the power output is affected by the speed shear but does not follow the power input variations (kinetic energy flux). One could wonder if the turbine simply averages the input speed profile and then gives the same power for a given non-uniform profile as for a uniform profile with a wind speed equivalent to the rotor averaged speed of the non uniform profile:

$$U_{eq} = \frac{1}{A} \int_{H-R}^{H+R} u(z)c(z-(H-R))dz \simeq \sum_i u_i \frac{A_i}{A}$$

where u_i is the horizontal wind speed at the ith height in the profile and A_i the area of the ith segment of the rotor swept area.

Figure 7 is similar to Figure 6 in that it shows the difference in power output obtained for a shear profile, except that now the reference power (P_0^{Ueq}) is that obtained for a uniform profile with the wind speed equal the rotor average wind speed from the sheared profile (U_{eq}):
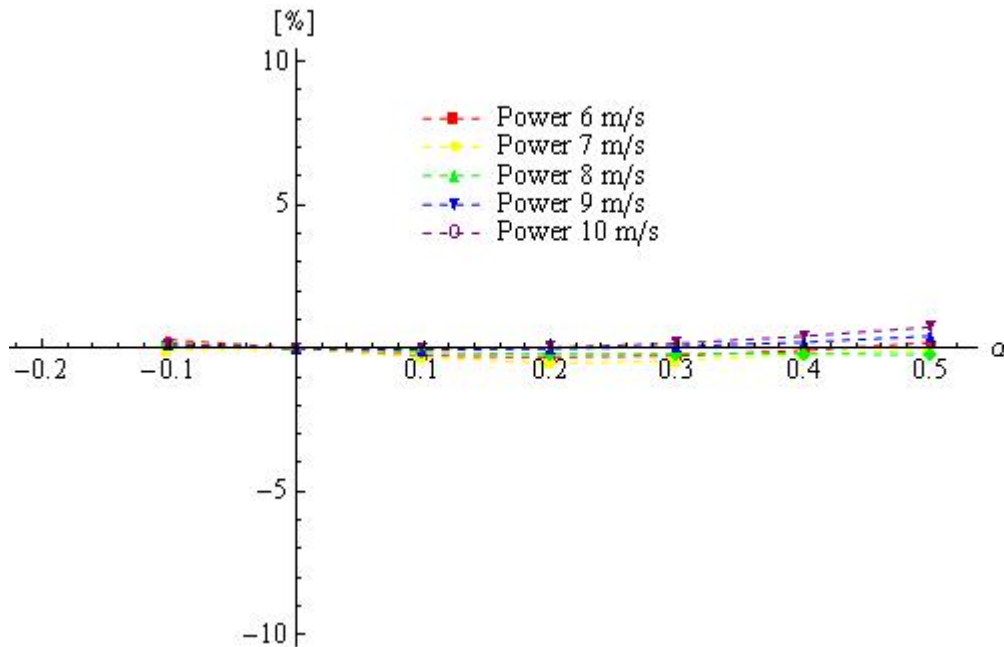

Figure 3. 7 Normalised difference between the power output obtained with a shear inflow and a uniform inflow (at the speed U_{eq}) as function of the shear exponent, for various wind speed at hub height. For the uniform inflow, the area averaged wind speed Ueq is used.

Since Figure 3.7 shows the results with the same plot range as Figure 3.6, we can see that the variation in power difference is much smaller in Figure 3.7. This indicates that, for these simulations at least, the power output obtained with a sheared inflow is much closer to the power output obtained with the uniform inflow at the rotor averaged wind speed P_0^{Ueq} than the power output $P_0^{u_{hub}}$ obtained with the uniform inflow with the same wind speed at hub height. However, if we look closer at Figure 3.7, we can see that the power output differences are not null, meaning that P is not equal to P_0^{Ueq}.

However the fact that this difference ($P - P_0^{U_{eq}}$) is close to zero is very probably the result of the assumptions made in HAWC2 as the torque coefficient (i.e. torque for one computational cell of the swept rotor area normalized with the dynamic force) is

normalized using the mean speed over the area (Bak, 2006). The fact that this difference is not exactly zero though may be due to the non constant induction factor in non uniform inflow.

3.4 Consequences on the power curve

A power curve shows the power output of the turbine as a function of the wind speed at hub height (IEC 61400-12-1). However, as shown previously, even for a constant hub-height wind speed, the power output of a turbine is expected to change with the wind speed shear. This results in large scatter in the power curve plot. Indeed, if we consider only the wind speed at hub height, all the points corresponding to profiles with the same wind speed at hub height appear with the same abscissa but with different ordinates as the different profiles result in different power outputs, see Figure 3.8.
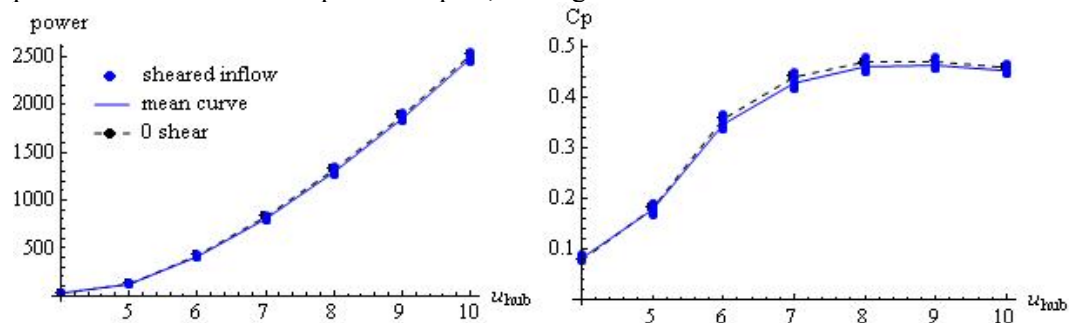

Figure 3. 8 Standard power curve and Cp curve, i.e. plotted as function of the wind speed at hub height and where only the wind speed at hub height is taken into account in the Cp evaluation. Results obtained for laminar flow with wind speed shear, same simulations cases as results shown in figure 3.6.

According to the results shown in 3.7, the use of a speed definition taking the wind speed shear into account instead of the wind speed at hub height could reduce the scatter. However the shear having two different kinds of effects on the power output of the turbine, it can be considered in different ways. Here, we suggest two definitions of equivalent wind speed:

❖ Average weighted with segment area: $U_{disk} = \sum_i u_i \frac{A_i}{A}$

❖ Kinetic energy flux approximation taking the vertical speed shear into account:

$$U_{KE} = \sqrt[3]{\sum_i u_i^3 \frac{A_i}{A}}$$

The simulated power curves obtained with those two equivalent wind speeds are shown in Figure 3.9.
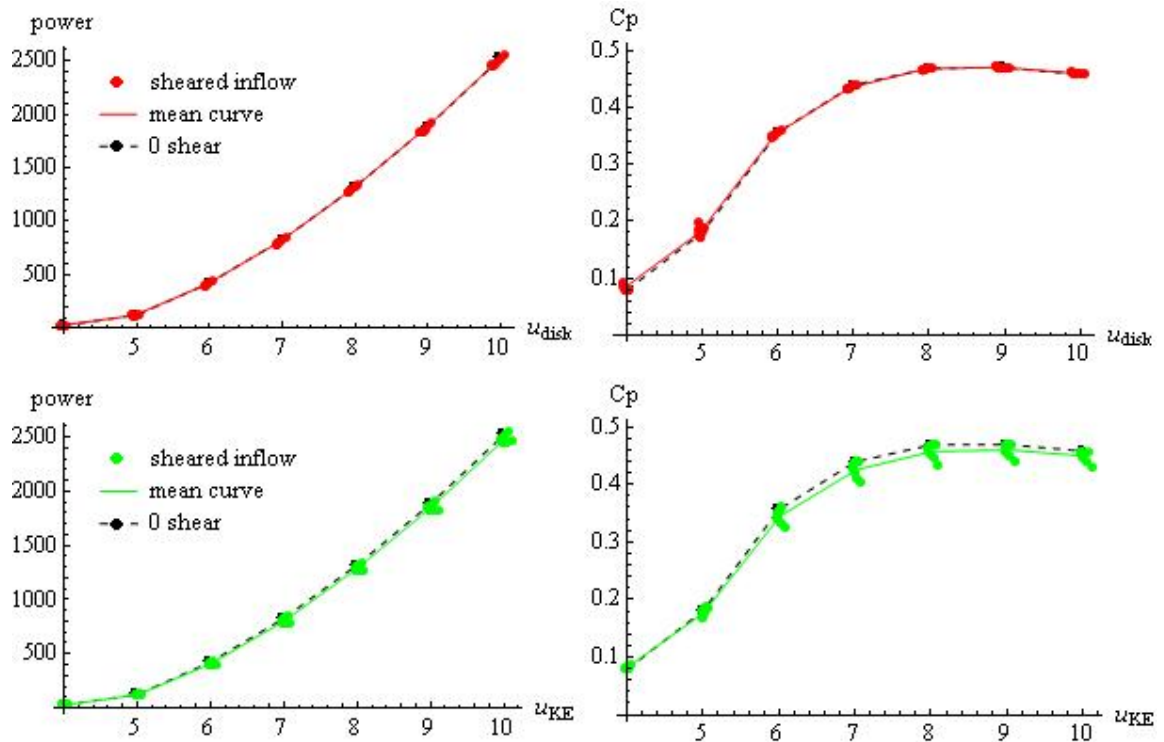
16

Figure 3. 9 Power curve and Cp curve obtained using different wind speed definitions in abscissa. Black points: points obtained for uniform inflow; dashed line: interpolation line considered as representation of the zero-shear power curve. Top: power as function of U_{disk}; Bottom: power as function of U_{KE}. The results shown in this figure were obtained with the same simulation cases as the results displayed in Figure 3.6 and Figure 3.8.

The reduction of the scatter corresponds to getting the points closer to the mean power curve. The idea of using an equivalent wind speed in the power curve is to get a new distribution of the points more consistent with the relation between the power input and the power output. However, the modification of the point distribution involves a modification of the mean power curve too. The quantification of the scatter is defined by the power mean residual error in each bin. The residual error of one single point corresponds to the (vertical absolute) distance between the point and the mean power curve. The mean residual error is the average of this quantity for all the points in the bin.

Based on those considerations, we can see that the first equivalent wind speed definition (U_{disk}) gives a mean power curve very close to the zero shear power curve and results in an obvious reduction of the scatter (the points are closely aligned with the mean power curve), however this is strongly suspected to be due to the approximation made in the aerodynamic model as explained previously.

The second definition (U_{KE}) gives a mean power curve similar to the mean power curve obtained with the wind speed at hub height. The scatter is obviously reduced for the shear exponent smaller than 0.3 (upper part of the C formed by the green dots in figure 3.10) but not for higher shear exponent. This is consistent with figure 3.6 as the kinetic energy flux decreases up to about $\alpha=0.3$ and then increases whereas the power output predicted by HAWC2Aero generally decreases while the shear exponent increases. On the other hand, using the second equivalent wind speed definition results in a way of plotting the power output of the turbine as a function of the power input. This could show the true efficiency of the turbine (as its ability to extract the power available in the wind). As we discussed already in (3.2), such a power curve remains shear dependant as the power extraction of a turbine is usually not optimized for sheared inflows. The controller sets the pitch angle and rotation speed in order to get a maximum C_p, but this is generally done based on measurements at the hub of the turbine. A cyclical pitch may result in a better

extraction of the available power and therefore in a reduction of the scatter due to the wind speed shear in the power curve.
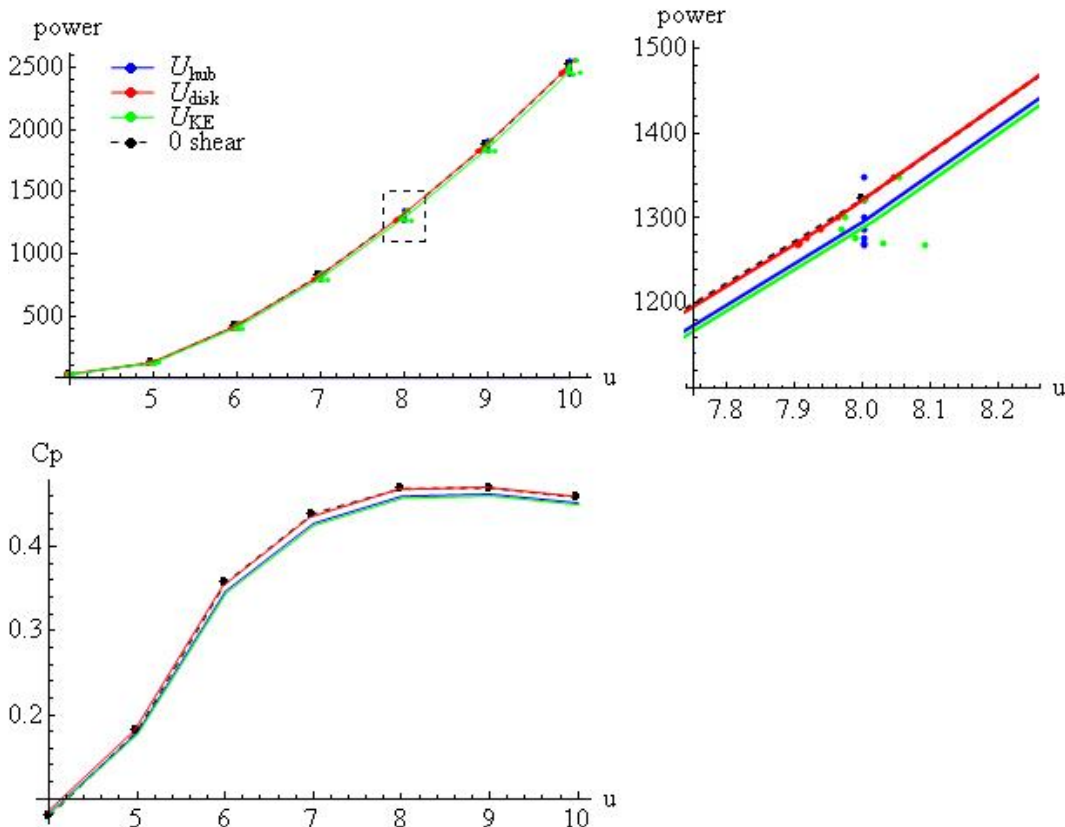

Figure 3. 10 (top, left) Scatter and mean power curve obtained for the various wind speed definitions: hub height speed (blue), U_{disk} (red) and U_{KE} in green together with the 0 shear power curve (dashed black); (top, right) Zoom in power curve figure around 8m/s at hub height; (bottom) Cp mean curves obtained for the different wind speed definitions.

3.5 Discussion about the wind speed shear effect

The shear effect can be seen as two effects:
1) A change in the power input (kinetic energy flux);
2) A cyclic variation of the inflow with the azimuth position of the rotor resulting in generally reduced ability to extract the available power (design optimized for uniform inflow).

Both those effects influence the power output, which results in a scatter larger than expected in the power curve if no additional information to the wind speed at hub height is taken into account. The use of an equivalent wind speed averaging the wind speed profile (or its kinetic energy) reduces the scatter. U_{disk} gave better results (smaller scatter) but it is very probably due to the way the local torque is normalized in HAWC2Aero. On the other hand, U_{KE} does not reduce the scatter as much as U_{disk} but its use in the power curve gives a direct representation of the efficiency of the turbine to extract the power available in the wind. Note that none of these equivalent wind speed definitions really account for the aerodynamics of the turbine in a non uniform inflow. Only an equivalent wind speed that accounts for the aerodynamic changes due to the sheared inflow would give a power curve independent of the wind speed shear. However this is very difficult (probably impossible)

to define, as it requires a full understanding the aerodynamics variation in an inflow with vertical shear, and this can vary from one single speed profile to another.

Both equivalent wind speed definitions, U_{disk} and U_{KE}, were used with experimental data (see second part of the report about experimental results). Both definitions resulted in the reduction of the scatter in the power curve but no significant difference was found between the scatter obtained with the different equivalent speeds.

4 Effect of the direction shear

4.1 Simple aerodynamics considerations
In order to illustrate the basic effects of the direction shear on the aerodynamics of the turbine, we consider here a linear variation of the angle between the turbine axis and the wind direction with altitude (no speed shear is assumed). The direction shear was implemented as a user-defined speed shear with variations in the two horizontal components of the wind vector (u_y=along the turbine axis; u_x= orthogonal to the turbine axis looking toward left):

$$\begin{cases} u_x = u_{hub} \sin(\alpha(z)) \\ u_y = u_{hub} \cos(\alpha(z)) \end{cases}$$

In comparison with speed shear, direction shear generates rather small variations of u_y but it also generates a variation of the horizontal component orthogonal to the turbine axis (whereas $u_x = 0$ in case of speed shear without direction shear). Figure 4.1 shows the profile of each Figure 4.1 shows the profile of each horizontal component of the free wind speed vector in front of the rotor in the case of a linear direction shear and of a power law speed profile.
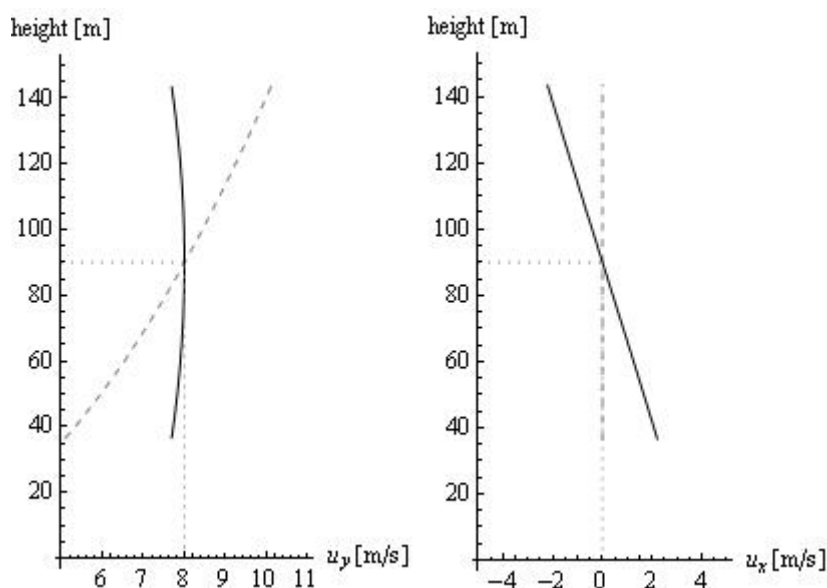

Figure 4.1 Profiles of the horizontal components of the wind speed (u_y on the left and u_x on the right) for a linear direction shear of 0.3 deg/m (in plain black) and in comparison, for a power law speed profile (no direction shear) in dashed gray.

Figure 4.2 shows the variations of each component of the free wind speed vector as seen from a point at 30m from the rotor centre and rotating at the same speed as the rotor in case of clockwise and anticlockwise direction shear.
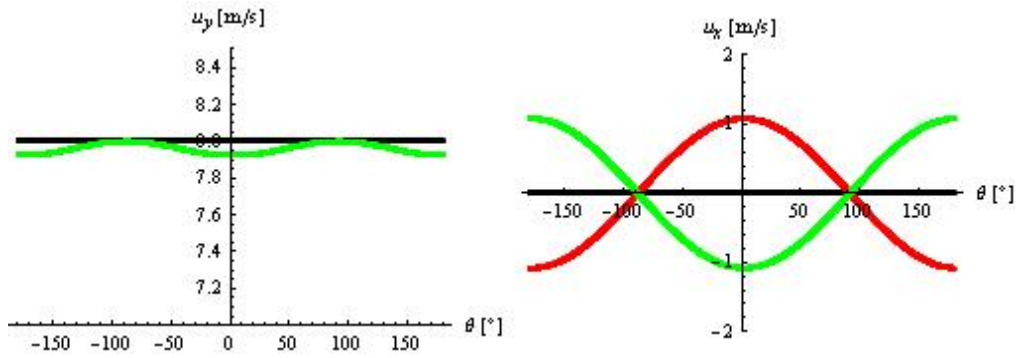
Figure 4.2 Horizontal components of the free wind speed seen from a rotating point, positioned at a radius of 30m, rotating at rotor rotational speed, as function of the azimuth angle: u_y *(left),* u_x *(right) . Green: Linear direction shear of -0.3 deg/m; Red: Linear direction shear of +0.3 deg/m; Black: no shear. (In all 3 cases the wind direction is aligned with the turbine axis at hub height.)*

When the point is at hub height, u_y is the same as in the uniform flow case. As soon as the point moves from this position (either upward or downward) u_y decreases as it follows the cosine of a small angler (which is null as hub height). As u_y is defined as the cosine of the angle, it is the same for negative and positive rotations of same the magnitude. On the other hand, u_x presents a pattern similar to the one of increasing wind speed with height described previously (one extremum at 0 deg and another one at 180 deg). In case of clockwise shear (veer), the speed vector rotates towards the right (Coriolis force in Northern hemisphere). In order to get a linear veer with zero degrees at hub height, u_x must be positive below hub height and negative above; and vice versa in the case of an anticlockwise shear.

Figure 4.3 shows the variations of the angle of attack and the relative speed seen by the blade at 30m radius for clockwise and anticlockwise direction shear. These parameters follow a pattern similar to u_y (extrema at 0deg and 180deg and opposite extrema at +/-90 degrees. However the deviations from the value at hub height are of opposite signs.
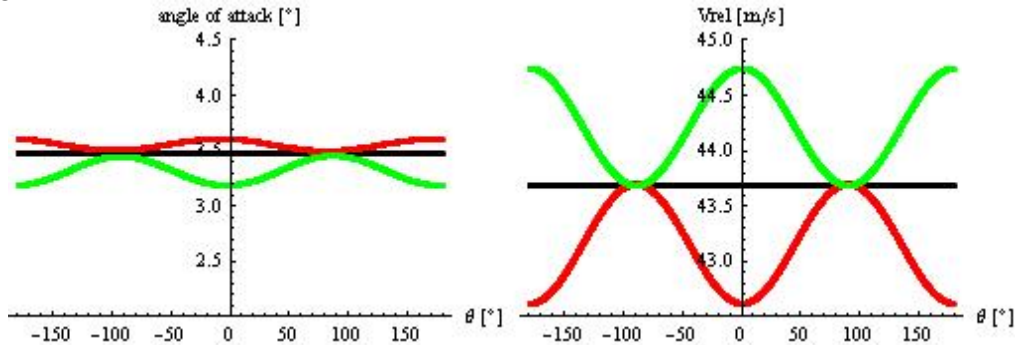

Figure 4.3 Angle of attack (left) and relative speed (including induction) (right) as a function of azimuth angle, seen from a point at radius r=30m on a rotating blade. Green: Linear direction shear of -0.3 deg/m; Red: Linear direction shear of +0.3 deg/m; Black: no shear. (In all 3 cases the wind direction is aligned with the turbine axis at hub height.)

The assumption has some consequences on the aerodynamics which in BEM is not accounted for. For azimuth positions other than horizontal directions modulation with the vector $\mathbf{\Omega r}$ occurs so that it is added with $u_x\mathbf{i}$. For $u_x\mathbf{i}$ positively in direction with $\mathbf{\Omega r}$, the vector sum is $|\mathbf{\Omega r}+ u_x |$, at a blade position opposite the arithmetic subtraction occurs. At horizontal positions, $\mathbf{\Omega r}$ and u_x are perpendicular. Flow along the blade $\sim\sin(\alpha(z))$ in

spanwise direction is assumed not to contribute with any lift or drag forces. This might be an incorrect assumption because of mass flow cause an effect. On the other hand centrifugal forces in effect with this mass would generate secondary flows changing the impact of forces. These effects would cause forces at $\pi/2 + \pi/2$ n, n $\in$ Z and change the harmonic variation to be unsymmetrical. However, presently these effects are neglected in the codes.

The angle of attack and the relative speed are affected by the induction but simple geometrical considerations (not taking the induction into account) can help to explain these variations, see Appendix A cases 3 and 4. For clockwise direction shear, the relative speed is smaller than the one for uniform inflow and the angle of attack is larger. It is the opposite in case of anticlockwise direction shear.

In a more advanced approach, we must consider that HAWC2Aero accounts for the variation of induction factor with azimuth position. The induction factor in a case of wind direction veer is therefore different from the induction factor obtained in uniform flow. This is why the angle of attack is actually not exactly the same at positions 90deg and 270 deg as in uniform flow.

It is interesting to look at the local forces as function of the azimuth angle, see Figure 4.4. Indeed the anticlockwise shear (green) results in variations opposite to the clockwise shear (red) since in the first case maxima are reached when minima are reached in the second case. Moreover, the opposite behavior for the angle of attack and the relative speed (see figure 4.3) results in dF_L variations of larger amplitude than for the clockwise case than for the anticlockwise case. Finally we can see that the local tangential force is slightly increased in the clockwise case and decreased for the anticlockwise case.
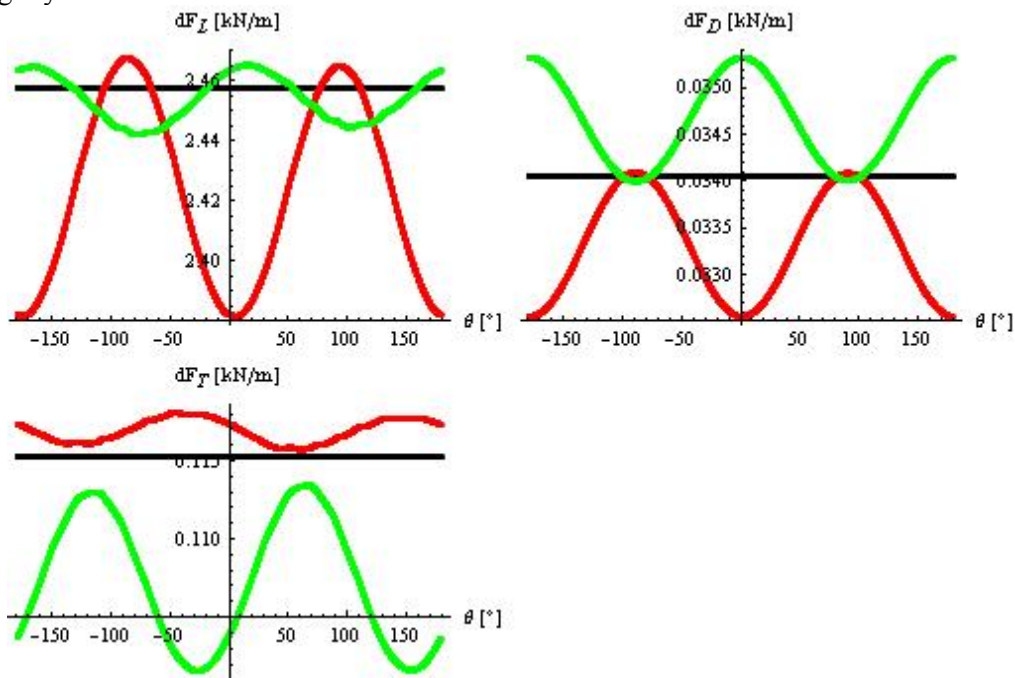

Figure 4.4 Local lift (top left), local drag (top right), local tangential force (bottom) seen from a point at radius r=30m on a rotating blade as a function of its azimuth position. Green: Linear direction shear of -0.3 deg/m; Red: Linear direction shear of +0.3 deg/m; Black: no shear.

4.2 Consequences on the power production
a) Isolated direction shear
In the theoretical case of isolated direction shear (no speed shear and laminar flow), we run simulations with linear direction shear between -0.3 deg/m and +0.3 deg/m and for a range of wind speeds at hub height from 5 to 10 m/s. Figure 4.5 shows the difference between the

power output obtained for a sheared profile and the power output obtained with a uniform inflow for the same wind speed at hub height ($P - P_0^{u_{hub}}$). In addition, Figure 4.5 shows the difference between the kinetic energy flux for power law profile and a constant profile ($KE_{profile}$-KE_{hub}).
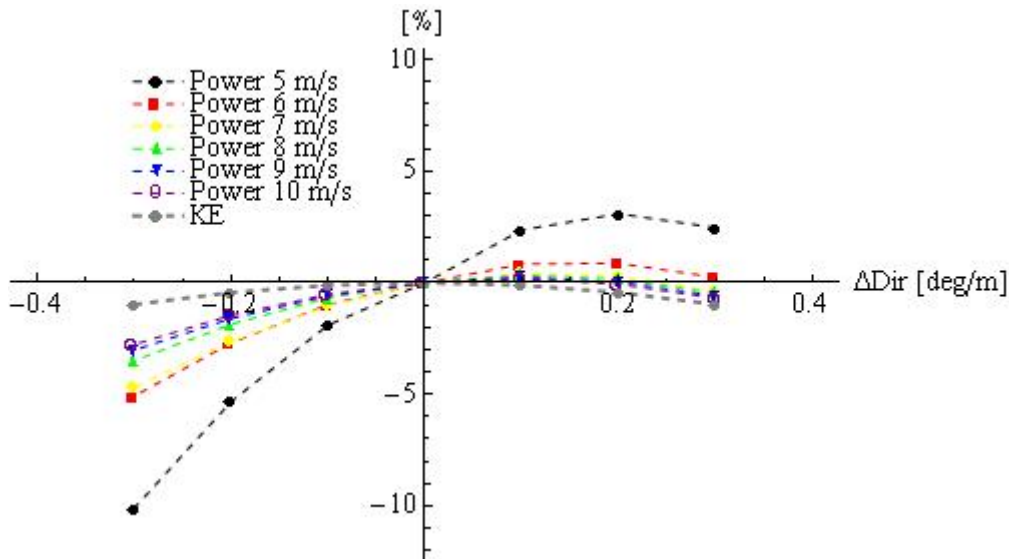

Figure 4.5 Normalised difference in kinetic energy flux (KE) and in power output between direction shear case and uniform case with u_{hub} as function of the direction shear gradient, for various wind speed at hub height.

Figure 4.5 shows several results:

1) When isolated, the direction shear has a smaller effect than the speed shear (when considering common values such as α=0 to 0.4 and Δdir= -0.3 to 0.3 deg/m), for most of the wind speeds. The largest decrease of power is obtained for large negative direction shear which are the less likely: negative/ anticlockwise direction shear is expected to happen less often than clockwise veer and with rather limited amplitude.

2) A direction shear does not have the same effect as a yaw error, as it is not symmetric around 0 degrees (Madsen, 2003). A small clockwise direction shear actually increases the performance of the turbine, whereas an anticlockwise direction shear systematically decreases the performance. (Walter 2007) explains this by an increase of the tangential force due to the increase in angle of attack for small positive direction shear.

Figure 4.6 shows the same results as figure 4.4 with in addition the quantities obtained for a clockwise direction of 0.1deg/m. We can see that the amplitude of the variations is smaller than for 0.3deg/m. The amplitude of the dF_T variations is similar for a radius of 30 but it is actually smaller for a radius of 40m with an averaged dF_T above the dF_T obtained for the uniform inflow (not shown here). As the torque results from the integration of the tangential force over the whole rotor swept area, this explains the power maximum (with a value above the power obtained for 0 shear) obtained for a small positive direction shear in figure 4.5.

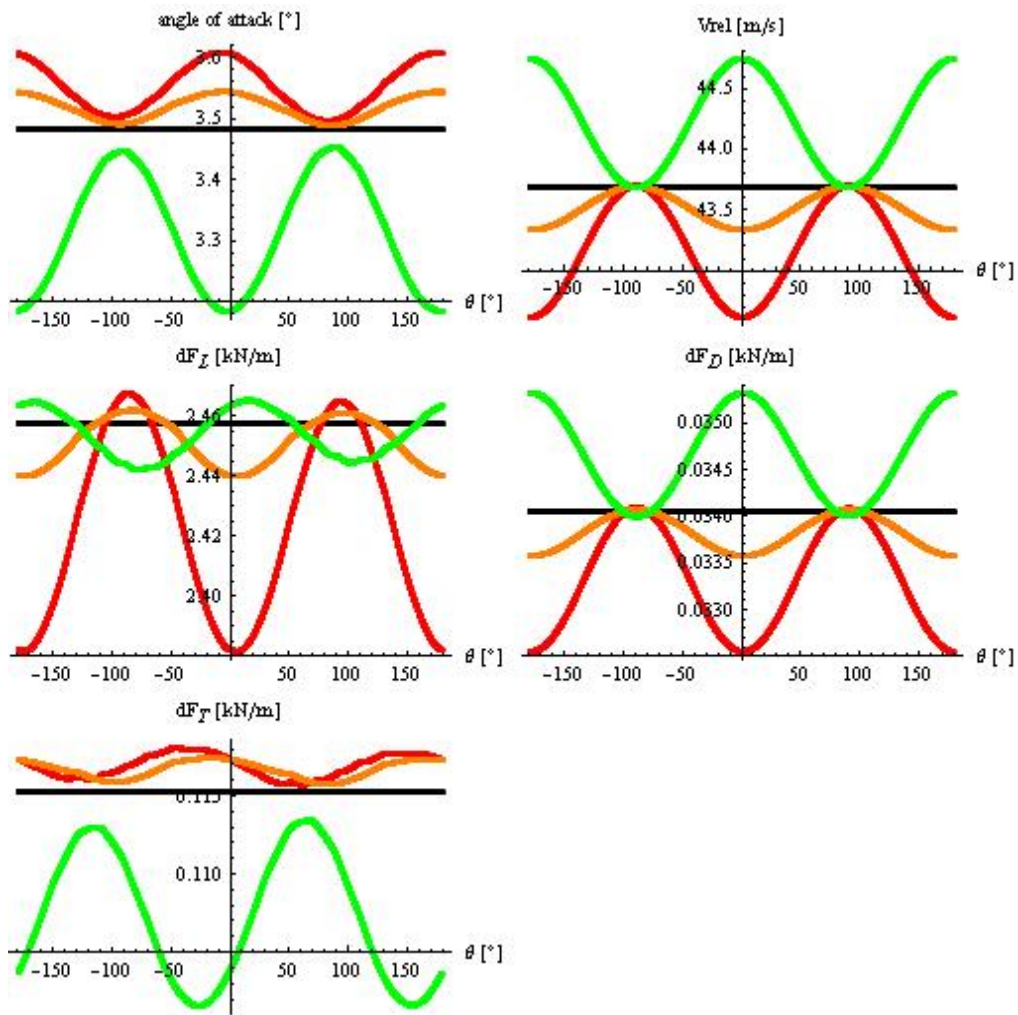*Figure 4.6   Angle of attack (top left), relative speed (top right), local lift (middle left), local drag (middle right), local tangential force (bottom) seen from a point at radius r=30m on a rotating blade as a function of its azimuth position. Green: Linear direction shear of -0.3 deg/m; Red: Linear direction shear of +0.3 deg/m; Orange: Linear direction shear of +0.1 deg/m; Black: no shear.*

b) Direction shear (linear) combined to speed shear (power law)

Figure 4.7 shows the net effect of wind veer and wind shear. An example of the difference in power output ($P - P_0^{u_{hub}}$) as function of speed shear coefficient for various direction shear values varying between -0.3 deg/m and +0.3 deg/m. For clarity of the figure, results are displayed for only one value of hub height wind speed: 8m/s.
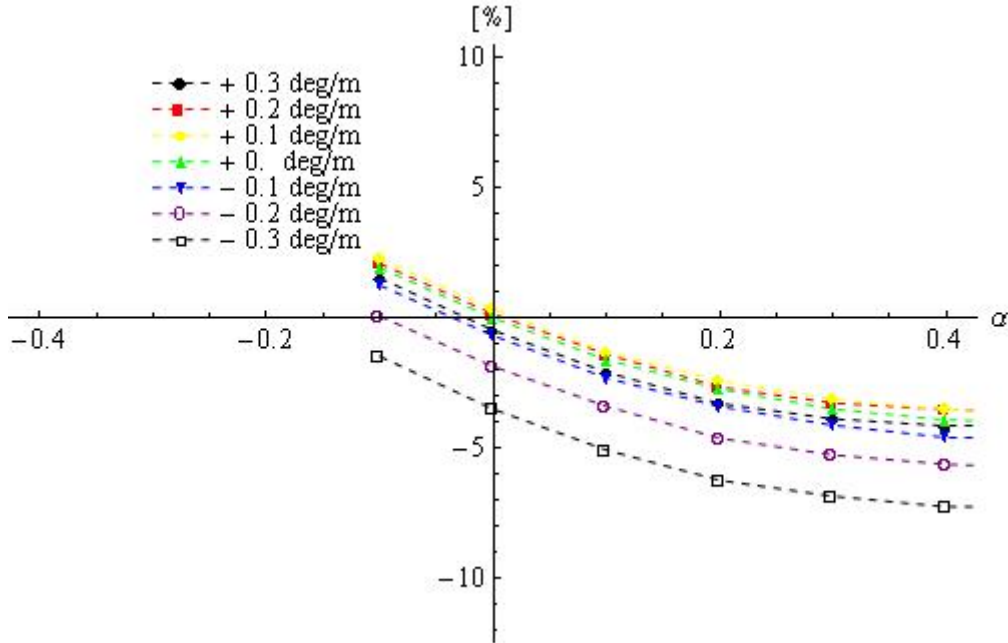

Figure 4.7 Normalised difference between the power output obtained with (combined speed and direction) shear and for uniform inflow (with the same u_{hub}) as a function of the speed shear exponent for various direction shear gradients.

Results from HAWC2Aero simulations show that when the direction shear was combined with speed shear, the power output reduction is larger than for isolated direction shear or isolated speed shear. However, this effect remains quite small (for moderate direction shear: between -0.1deg/m and +0.3 deg/m). Note that for clockwise veer (occurring the most), the power is actually increased compared to 0 veer cases but not as much as it is decreased by the speed shear.

4.3 Consequences on the power curve

We run simulation cases with both speed and direction shear (and laminar flow) for various wind speed at hub height. The outputs from those simulations were used to plot the power curve using different wind speeds in abscissa, see Figure 4.8. First, Figure 4.8 (Top) shows the standard power curve where the power is plotted versus the wind speed at hub height. Again, in each wind speed bin, as the wind speed at hub height is the same but the power output is altered by the direction shear, it results is some scatter.

Secondly, the power is plotted as a function of the equivalent wind speed defined in section 3.5, U_{disk} and U_{KE}, in figure 4.8. (middle left) and (bottom left) respectively. The difference with Figure 4.8.a results from the decrease of the scatter due to the speed shear. Scatter within cases with direction shear but no speed shear (displayed in green) has not changed. Indeed, in the case of direction veer, the horizontal wind speed magnitude is the same at all heights, since the vector is simply rotating. Therefore any of the previously defined equivalent wind speeds are equal to the hub height wind speed.

However the previous analysis of free and relative wind speeds as functions of the azimuth angle leads to the suspicion that the component of the wind along the axis has the biggest impact on the rotor aerodynamics. Therefore we could adapt the equivalent wind speed definition by using the component u_y instead of the horizontal wind vector norm ($\|u\| = \sqrt{u_x^2 + u_y^2}$).

$$U_{disk\_proj} = \sum_i (u_i)_y \frac{A_i}{A}$$

$$U_{KE\_proj} = \left(\sum_i (u_i)_y^3 \frac{A_i}{A} \right)^{1/3}$$

where $(u_i)_y$ is the horizontal component of the wind normal to the rotor plan at the ith height in the speed profile.

(Note in the case of wind speed shear without direction shear, $u=u_y$.)

These new definitions of equivalent wind speed reduce the scatter in the power curve as shown in figures 4.8 (middle right) and (bottom right). The variation of the u_y is so small that U_{disk_proj} and U_{KE_proj} give very close values.

Note that these equivalent wind speeds assume a cosine variation. As the yaw error was found to follow a cos^2 pattern (Petersen, 2004), it is often suggested to use a cos^2 in the definition of equivalent speed. However both the functions cos and cos^2 are even functions, therefore none of them can give the asymmetry seen in Figure 4.4.
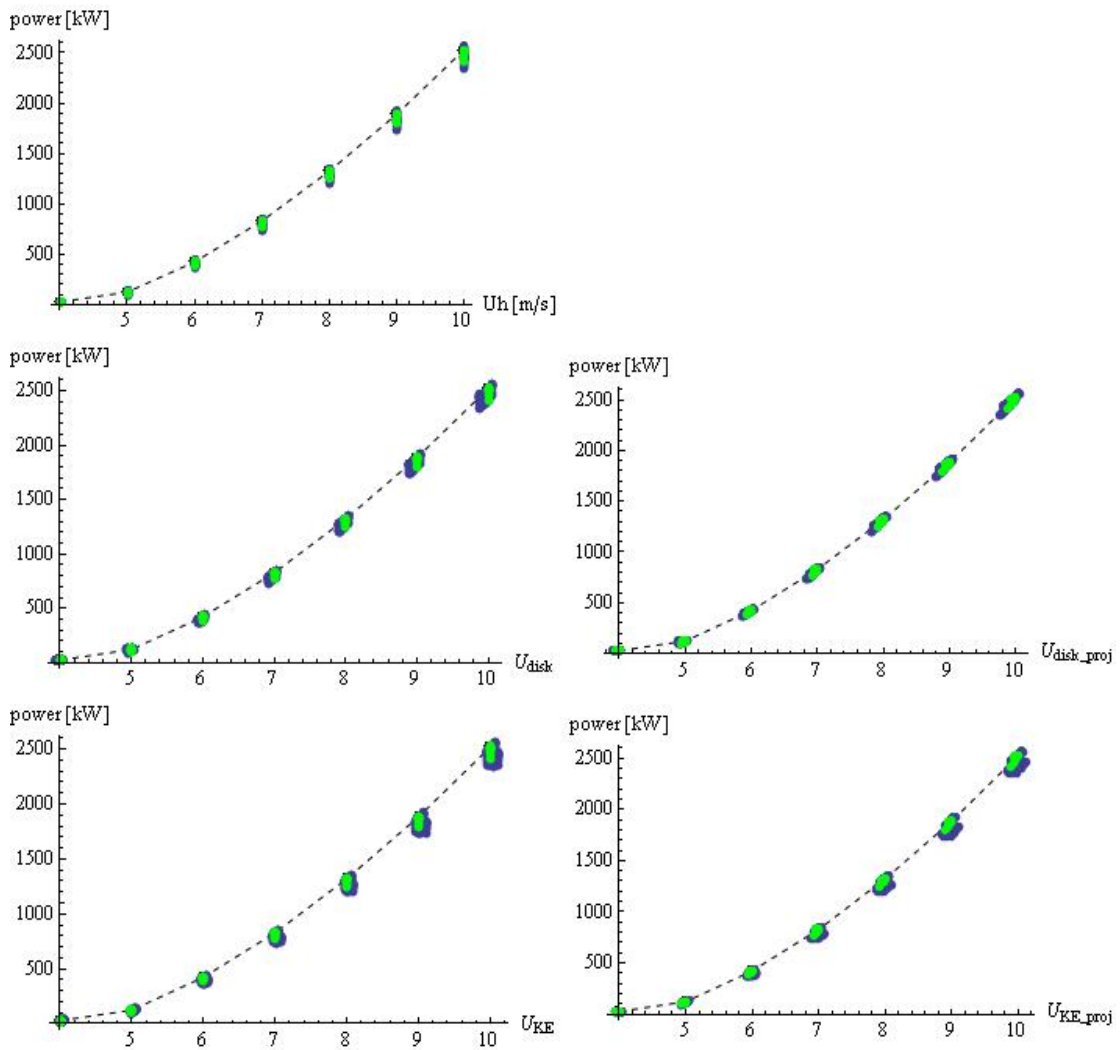
Figure 4.8 Power curve scatter plots obtained for laminar flow with various wind speed shear and direction shear using different wind speed definitions in abscissa. Black points: points obtained for uniform inflow; dashed line: interpolation line considered as representation of the zero-shear power curve, Blue dots: power output obtained with linear direction profiles and power law speed profiles; Green dots: power output obtained with linear direction profiles and no speed profiles. Top: power as function of the wind speed at hub height; Middle Left: power as function of U_{disk}; Middle Right: power as function of U_{disk_proj}; Bottom Left: power as function of U_{KE}; Bottom Right: power as function of U_{KE_proj}.

Note that the results displayed with green dots in Figure 4.8 were obtained with the same simulations cases as the results displayed in figure 4.5,

4.4 Discussion about the direction shear effect

The direction shear also results in a cyclic variation of the loads on the blade as it rotates. The main difference with the speed shear effect is that the direction shear implies a variation of the horizontal component of the wind orthogonal to the turbine axis (u_x). A clockwise direction shear results in a higher local tangential force than an anticlockwise direction shear. A small clockwise direction shear could even give more power than a uniform inflow, according to the simulations. In return, any negative direction shear results in a decrease of the power output. However negative wind direction shears occur much less frequently than positive shear.

According to these simulations results, for typical values, the direction shear has a smaller effect on the turbine power output than the speed shear. However, the effect is increased when both phenomena are combined.

5 Effect of turbulence intensity

Until now, we have only considered laminar inflow in order to isolate the effect of speed and direction shear. In reality though, the inflow is not laminar, and a turbine is subjected to the combined effect of shear and turbulence. Therefore we investigated how large the effect of turbulence is in comparison with speed and direction shear.

As explained in section 2, wind speed time variations are simulated with the Mann model of turbulence which creates statistical turbulence with a realistic temporal and spatial structure. In order to obtain statistically significant results, each shear case is run with 10 different time series created by the Mann model using different seeding. In all simulations presented here, the turbulence intensity is assumed constant with height, in order to focus on the effect of shear.

5.1 Simple aerodynamics considerations
a) Isolated turbulence (no shear)
In this section we show results from simulations using a statistically uniform flow (i.e. same average and standard deviation everywhere with a turbulence intensity of 10%. Figure 5.1 shows the time series of the wind speed at 3 points at 3 different heights observed from a stationary frame of reference. We can see that the wind speed varies with time at all points and is not exactly the same at all three points at each time but the mean wind speed is the same and the standard deviation similar.
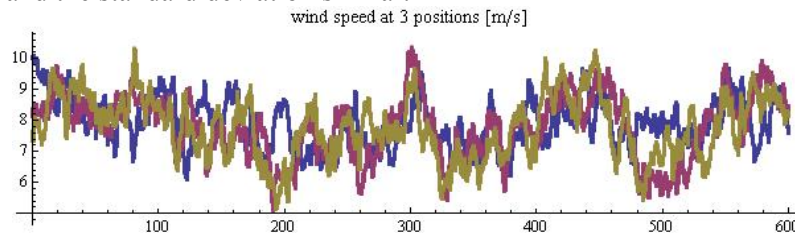

Figure 5.1 Time series of the axis-wise component of the wind speed (u$_y$) from a fixed point at hub height (blue), at lower tip height (red) and higher tip (yellow).

Figure 5.2 (top) shows the free wind speed but from a point rotating at the same speed as the rotor. Higher variance is added by the rotational sampling of the wind speed as the point repeatedly passes through coherent structures. This larger variance is consequently also evident in the angle of attack variations (see Figure 5.2(bottom)).
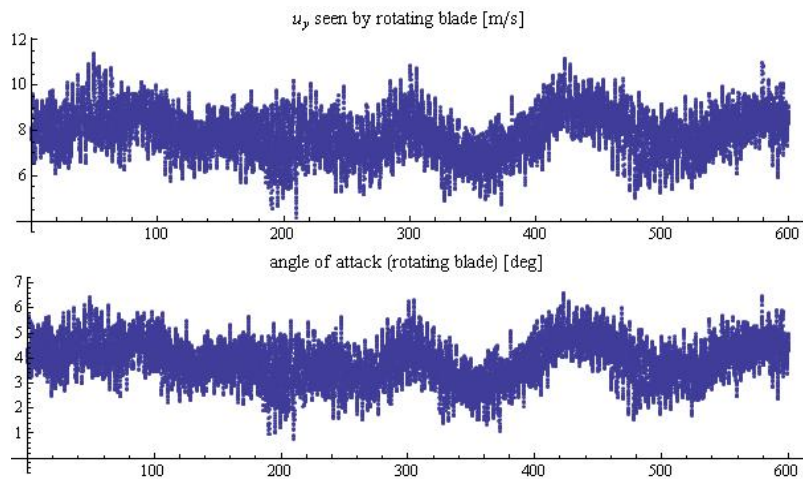
Figure 5.2 (Top): Time series of the axis-wise component of the free wind speed (u_y*) from a rotating point at a radius of 36m from the rotor center. (Bottom): Times series of the angle of attack from r=36m on a rotating blade.*

5.2 Consequences on the power curve

Increasing the wind speed standard deviation (turbulence intensity) results in increasing the power standard variation and therefore the scatter in the power curve, see Figure 5.3.
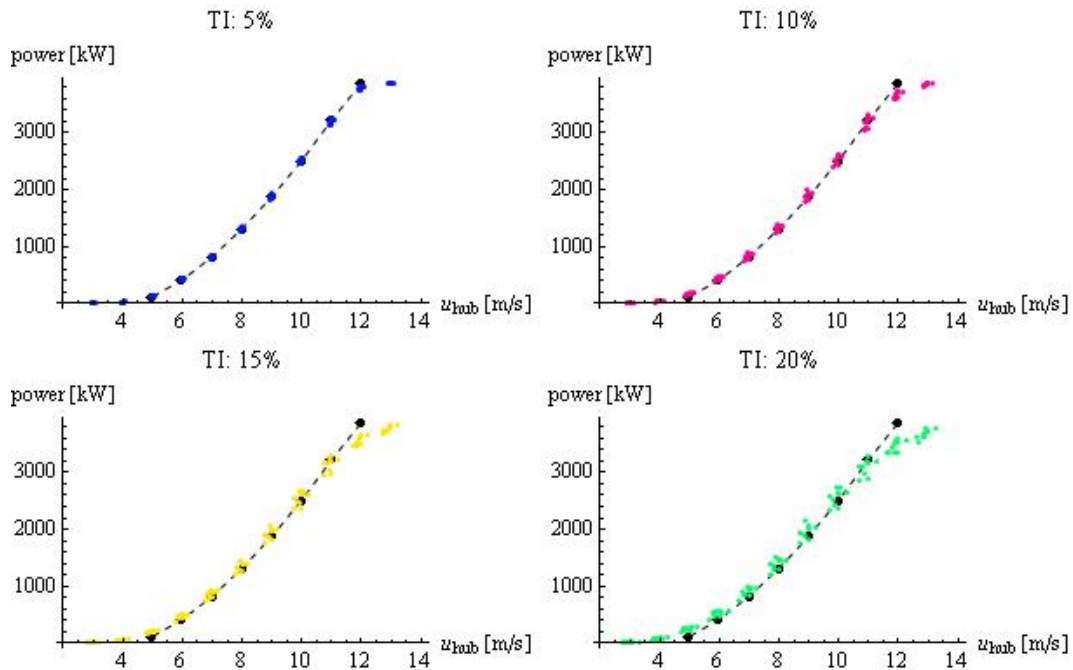

Figure 5.3 Power curve scatter plots obtained for various turbulence intensities from 5% to 20%. Black points: points obtained for uniform inflow; line: interpolation line considered as representation of the zero-turbulence power curve; colored dots: points obtained for turbulent inflow. The scatter increases with the turbulence intensity.
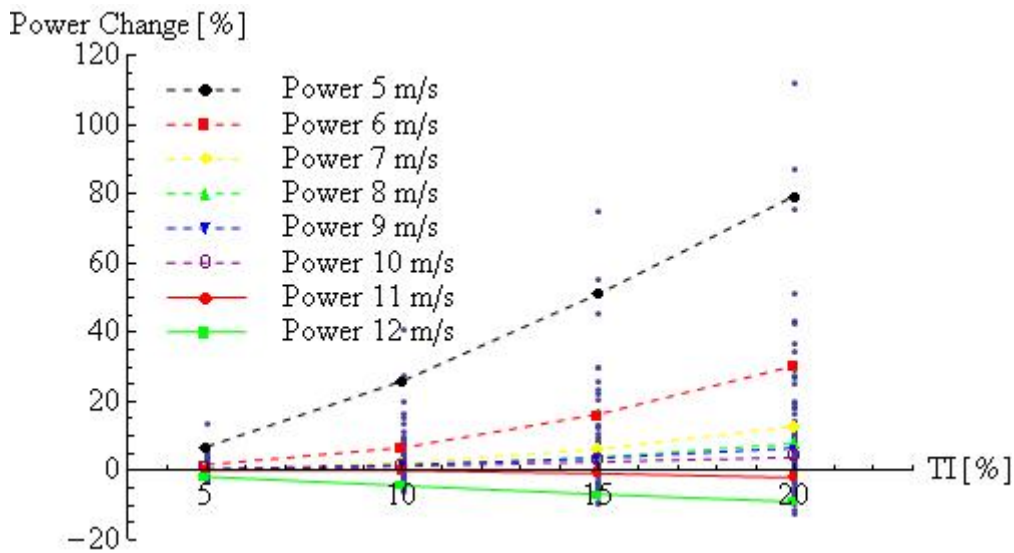
Figure 5.4 Normalised power difference between turbulent and laminar inflow as function of the turbulence intensities for various wind speed. The small dots represent all simulations cases (various mean speeds and turbulence intensities). The larger markers show the average per wind speed per turbulence intensity. The lines correspond to the interpolation between those average points.

As the wind speed fluctuates around the rated wind speed, the power extracted is limited to the rated power. Therefore only "negative fluctuations" (i.e. when the instantaneous speed is below rated speed) of the wind are transformed into power fluctuations. Consequently, 10 minutes mean power obtained with a given turbulence intensity is generally smaller than the power that would be obtained with the same mean wind speed and a laminar flow (TI=0%), and the mean power decreases as the turbulence intensity increases (Kaiser 2003, Albers 2007), see Figure 5.5. In the same way, as the wind speed fluctuates around the cut-in wind speed, only the positive fluctuations are transformed in power fluctuations. Therefore, near the cut-in wind speed, the mean power is expected to increase with the turbulence intensity.
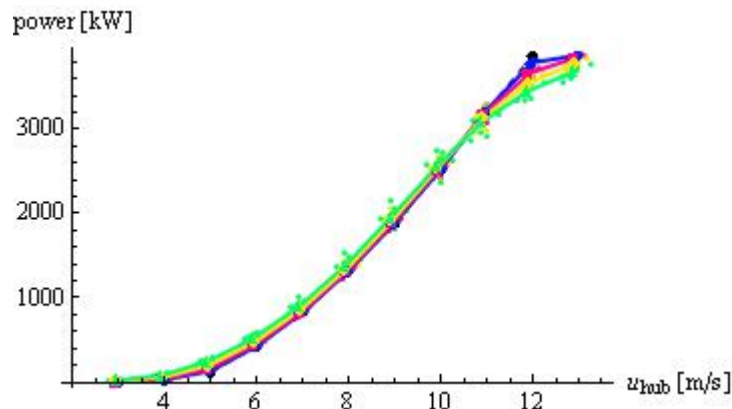

Figure 5.5 Average power curves for various turbulence intensities (5% (blue), 10% (red), 15% (yellow), 20% (green))

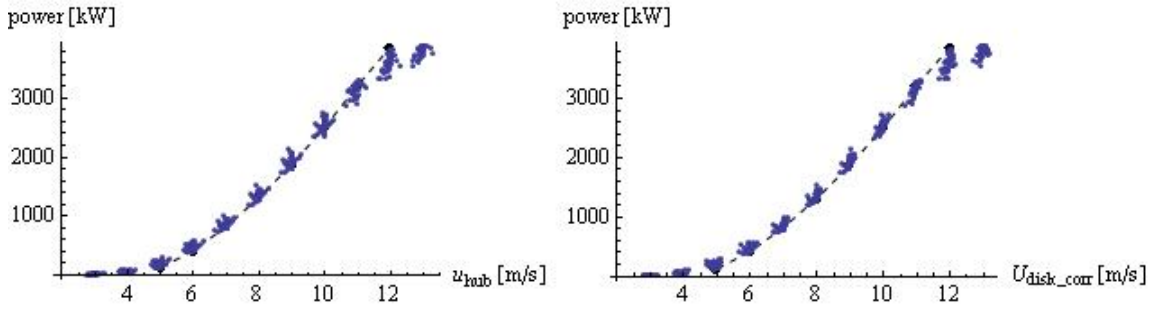*5.3 Note on equivalent wind speed and turbulence*

Figure 5.6 Power curve scatter plot obtained with the output of the simulations cases with turbulence (all TI together) and no shear: power as function of the hub height wind speed (left), power as function of U_{disk_proj} *(right).*

In comparison with the power curve plotted as a function of the hub height wind speed u_{hub}, when plotted as a function of the equivalent wind speed U_{disk_proj} we can actually observe a small reduction in the scatter, see Figure 5.6. This is because, although we are using a nominally uniform profile as model input, the effect of the turbulence is to actually generate slightly non-uniform mean shear profiles, see Figure 5.7. As we have seen previously, with most non-uniform profiles, the power correlates better to the equivalent wind speed than to the hub height wind speed.
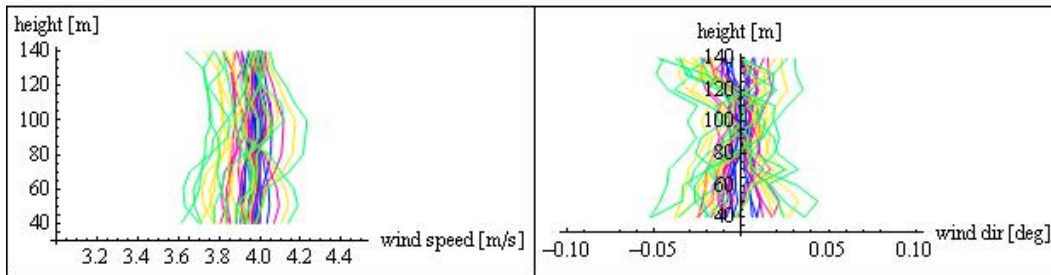

Figure 5.7 Output wind speed profiles (left) and direction profiles (right) for the uniform wind speed profile at 4m/s (no speed shear, no direction shear).

However the equivalent wind speed definitions proposed previously in this report cannot reduce the scatter due to the turbulence itself since they are based on 10 minutes mean speeds.

5.4 Equivalent wind speed including the turbulence intensity

The effect of turbulence intensity can be taken into account in the equivalent wind speed based on the kinetic energy flux by introducing the extra kinetic energy introduced by the turbulence.

A Taylor development of the cube of the wind speed gives:

$$u^3 = (\langle u \rangle + u')^3$$

$$= \langle u \rangle^3 + 3\langle u \rangle^2 u' + 3\langle u \rangle u'^2 + u'^3$$

Now if we consider the 10 minutes average of the cube of the wind speed, the second term disappears by definition of the fluctuations and the last term disappears if the fluctuations distribution is assumed to be Gaussian:

$$\langle u^3 \rangle = \langle u \rangle^3 \left(1 + 3 \frac{\langle u'^2 \rangle}{\langle u \rangle^2} \right)$$

$$= \langle u \rangle^3 \left(1 + 3 \frac{\sigma^2}{\langle u \rangle^2} \right)$$

We can see that the 10 minute average of the kinetic energy flux actually increases with the turbulence intensity ($TI = \dfrac{\sigma}{\langle u \rangle}$ where σ is the horizontal wind speed standard deviation and $\langle u \rangle$ the mean horizontal wind speed):

$$\langle KE \rangle = \frac{1}{2} \rho \langle u^3 \rangle A$$

$$= \frac{1}{2} \rho \langle u \rangle^3 \left(1 + 3 TI^2 \right) A$$

We could then define a new equivalent wind speed:

$$U_{eq\_TI} = \left(\sum_i \langle u_i \rangle^3 \left(1 + 3 \frac{\sigma_i^2}{\langle u_i \rangle^2} \right) \right)^{1/3}$$

The problem is then that U_{eq_TI} simply increases with the turbulence intensity whereas the turbine power output does not when getting close to the rated power, see Figure 5.8. A better result could be obtained if the bends of the power curve were taken into account as suggested in (Kaiser, 2003).
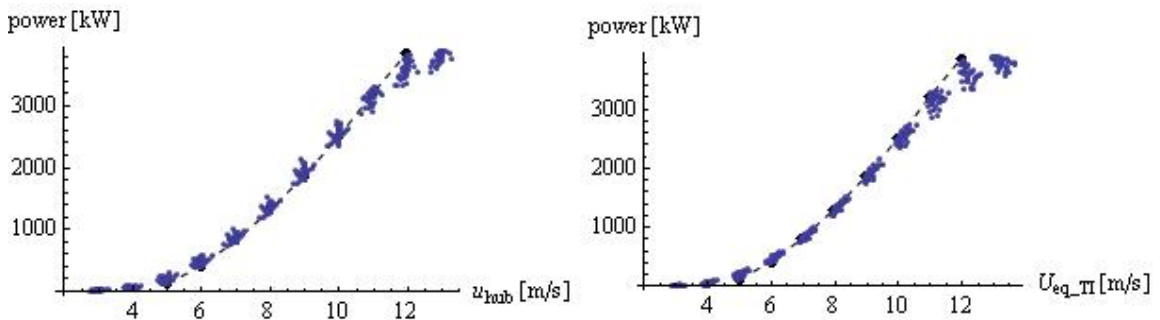

Figure 5.8 Power curve scatter plot obtained with the output of the simulations cases with turbulence (all turbulence intensities together) and no shear: power as function of U_{disk_proj} *(left), power as function of* U_{TI} *(right).*

It seems that turbulence cannot be simply accounted for with a simple equivalent wind speed as we did for shear. As one of the problems is the averaging over 10 minutes, better results are expected by considering fast data (Gottschall, 2009) but this requires a rather more complex method not necessarily suitable for the applied purpose of power curve verification. The most suitable method so far for this purpose is (Albers, 2007). Albers' method is meant to solve the problem due to the 10 minutes averaging for various turbulence intensities. This method is based on the fact that the 10 minutes average of the power is not linearly related to the 0 turbulence mean wind speed. In Albers' method, the 10 minutes power average depends on the wind speed distribution during the considered 10

minutes (it is assumed Gaussian) and the shape of the power curve. If the shape of the power curve we would get for 0 turbulence intensity was known, it would then be possible to calculate the 10 min mean power that would be obtained with a given turbulence intensity (>0%) as it only changes the wind speed distribution. Albers'method is therefore made of 2 steps:

1) The estimation of the 0% turbulence intensity power curve;
2) The simulation of the power curve we would obtain for chosen turbulence intensity.

It should be noted that , 1) Albers' method takes only the wind speed at hub height into account; 2) contrary to the equivalent wind speed method which modifies the wind speed definition (therefore influences the x-axis) of the power curve, Albers' method changes the power value (the y-axis).

5.5 Turbulence and shear

We now consider a turbulent inflow with a turbulence intensity of 10%, with a mean wind speed profile following the power law with a shear exponent of 0.5.

a)Aerodynamics

Figure 5.9 shows the time series of the wind speed at three heights. The effect of speed shear is that the wind fluctuates around three different mean values (for the three different heights), in contrary to the turbulent uniform inflow where the three time series overlapped each other (Figure 5.1). The consequences are an increase of the fluctuation amplitude seen by the blade and in the angle of attack, see Figure 5.10.
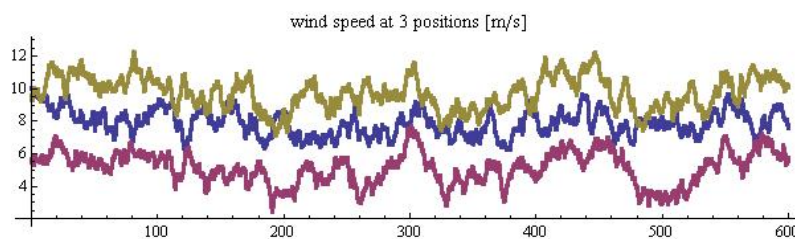

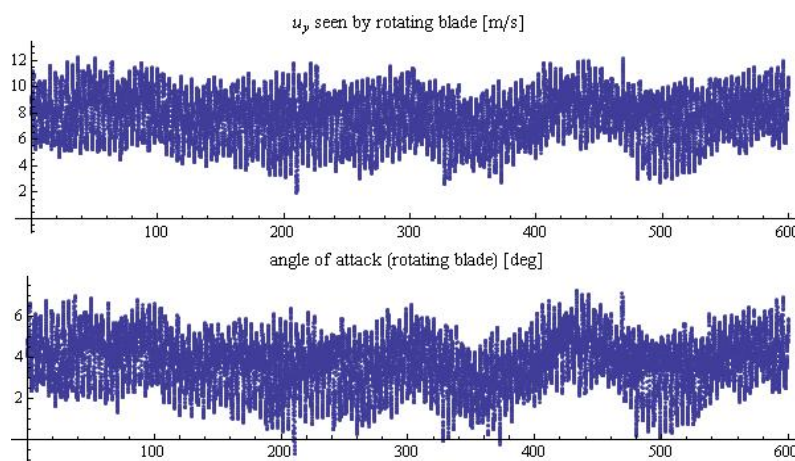*Figure 5.9 Time series of the wind speed at hub height (blue), at lower tip height (red) and higher tip (yellow).*

Figure 5.10 Times series of the u_y and angle of attack seen from r=36m on a rotating blade

If we plotted the axis-wise free wind speed as a function of the azimuth angle (as done in the shear analysis) we could observe cyclic variation due to instantaneous shear if only one or a couple of rotations were considered. However if 10 minutes were considered, then the speed profiles succeeding each other get all mixed up and no cyclic pattern is brought out (not shown).

In Figure 5.11, we plotted the axis-wise free wind speed as a function of the azimuth angle (as done in the shear analysis). The cyclic fluctuation of the speed seen from a rotating point appears clearly in spite of the random fluctuations due to the turbulence. This shows that, even though the scatter due to turbulence can be larger than the scatter due to shear, the shear effect is not overwhelmed by the turbulence. Of course, this is relative to the shear and turbulence magnitudes. However, within the assumption of flat terrain, the turbulence intensity is limited and only a few values exceeding 15% are expected (based on westerly wind observation at Høvsøre). Moreover high shear is generally expected in conjunction with a stable boundary where the turbulence intensity would generally be low.
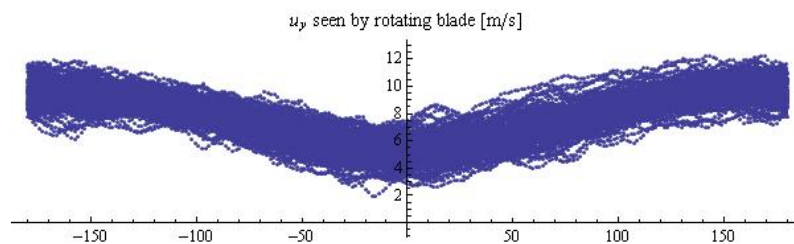

Figure 5.11 u_y *seen from rotating blade*

b) Power curve

In order to get a first impression of the effect of shear profile with different turbulence intensities, simulations were carried out for several power law profiles (shear exponent between -0.1 and 0.5) with a hub height wind speed of 8m/s (as input) with 10% and 20% turbulence intensity.
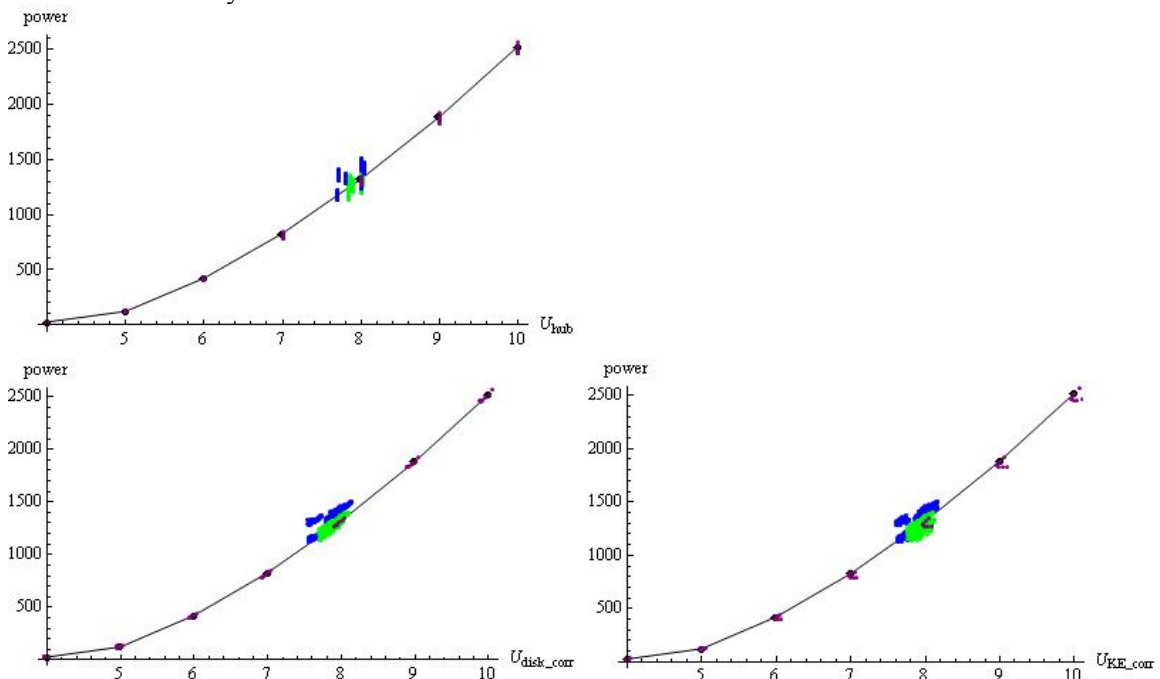

Figure 5.12 Part of power curves obtained for shear and turbulent inflows. (a): power as function of hub height; (b): power as function of Ueq_disk; (c) power as function of Ueq_KE

As the effect of turbulence does not overwhelm the effect of shear, the use of an equivalent wind speed taking the shear into account still results in the decrease of the scatter (due to wind shear). The reduction is smaller because of the remaining scatter due to the turbulence. Indeed the groups of points (for 10% and 20% turbulence intensity) remain quite distinct. If the turbulence intensity groups are considered separately, as the scatter decreases, the points converge toward different power curves (depending on the turbulence intensity as seen in Figure 5.6).

5.6 Discussion about the turbulence intensity effect

The effect of turbulence is more complex than that for shear and it is therefore more difficult to account for in the power curve. However, in moderate levels of turbulence, the cyclic variation caused by the speed shear dominates the turbulent inflow and the equivalent speed methods can still reduce the scatter in the power curve.

The main problem influencing the power curve is actually the 10 minutes averaging of the wind speed and the power. We can distinguish 2 effects:

1) Turbulence increases the 10 minutes mean kinetic energy;
2) The 10 minutes mean power does not follow the 10 minutes mean kinetic energy as the instantaneous power output is not a linear function of the kinetic energy. Indeed, the power averaging effect on the power curve is more pronounced where the Cp varies a lot, like near cut-in and rated wind speeds.

It would be interesting to combine the equivalent wind speed method and the Albers' method. This combination may result in a reduction of the scatter.

6 Realistic shear with standard turbulence

Now that the effect of speed shear, direction shear and turbulence intensity, as well as some combinations of these parameters have been described, more realistic inflows were simulated. Indeed, the power law profile is a common model for the wind speed profile but it is not representative of all kinds of profiles that can occur over flat terrain.

We selected various speed profiles from measurements obtained with the meteorological mast at Høvsøre within the year 2007. These profiles were selected according to their shape and their kinetic energy flux in order to obtain a selection as various as possible (see appendix).

These profiles were used as mean speed profile inputs for the aerodynamic model. Turbulence fluctuations were added to the profiles. As the main objective of the overall work presented here is to investigate the influence of the shear, the turbulence intensity given as input was based on the IEC standard 61400-12-1 definition:

$0.16 (0.75\, u_{hub} + 5.6)$. As explained in section 5, each inflow (here described by a wind speed profile and a turbulence intensity) was run with 10 different time series for statistical consistency (it reduces the sampling standard deviation by $\sqrt{10}$).

These cases were simulated with two aerodynamic models:
- HAWC2Aero, already described in 2;
- Vestas model (shortly described in 6.b)

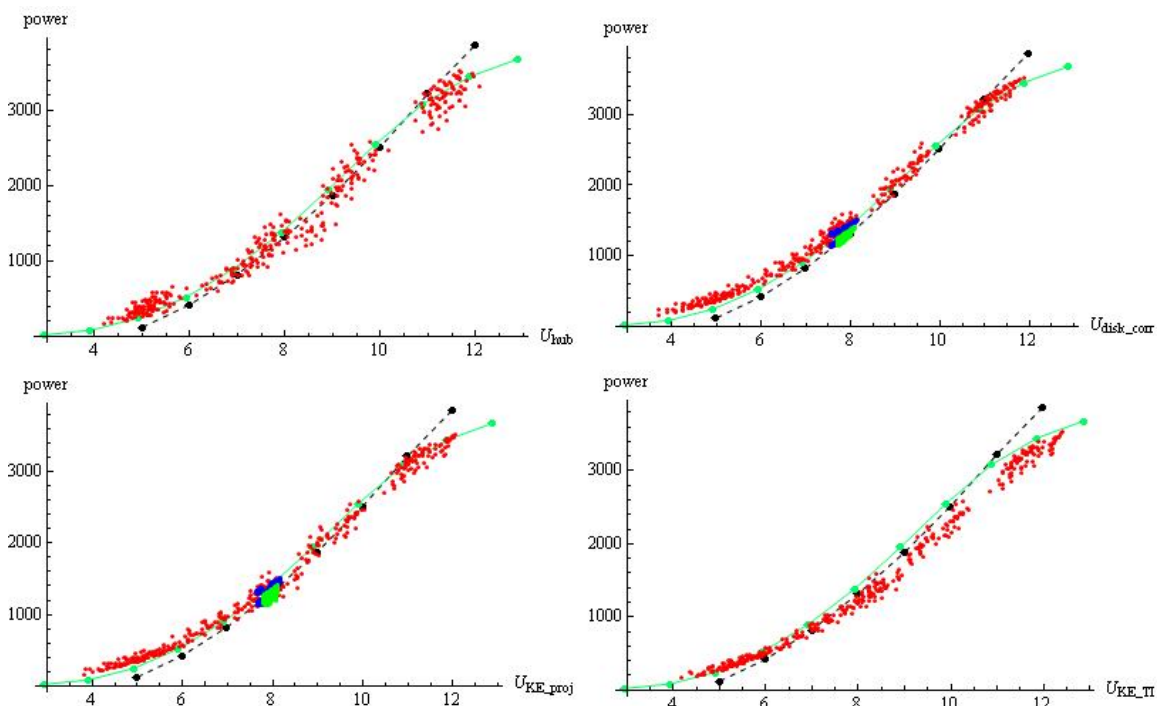*a) HAWC2Aero (Risø DTU) _ Simulations for 3,6 MW Siemens wind turbine*

Figure 6.1 Power curve scatter plots obtained for turbulent and shear inflow using different wind speed definitions in abscissa. Black points: points obtained for uniform inflow; black dashed line: interpolation line considered as representation of the zero-shear zero-turbulence power curve, Red dots: power output obtained with turbulent shear inflow; Blue and Green dots: same as figure 5.10. Top Left: power as function of the wind speed at hub height; Top Right: power as function of U_{disk_proj}; *Bottom Left: power as function of* U_{KE_proj}, *Bottom Right: power as function of* U_{KE_TI}.

Figure 6.1(top left) shows the standard power curve scatter plot (i.e. the power as a function of the wind speed at hub height). The scatter is very large. This is partly due to the turbulence intensity definition that gives very high turbulence intensity of about 20% which is considerably larger than the typical values offshore or in flat terrain (measurements give a turbulence intensity of about 7% in average).

We can see a clear reduction of scatter when using an equivalent wind speed accounting for the wind speed shear (both definitions), see Figure 6.1 (top right and bottom left). The remaining scatter is probably due to the turbulence. The reduction of scatter does not converge towards the 0-shear 0-turbulence power curve, but towards power curve 0-shear & 20% TI (displayed by a green line).

Finally, in Figure 6.1 (bottom right), we can see that the equivalent wind speed reduces the scatter as much as U_{KE_TI}, but modify the shape of the mean power curve as for the same power, U_{KE_TI} is larger than U_{KE_proj}.

b) Vestas simulations
The turbine simulated here was a generic pitch regulated turbine model with a 100m diameter rotor and 80 meter tower.
The program used for the simulations is VTS which is based on Flex5 (BEM model) with some non-fundamental modifications/enhancements made in-house.

The same input as above (realistic shear and standard turbulence intensity) were used. For each input case, 6 simulations were run in order to get statistically significant results and were then averaged.
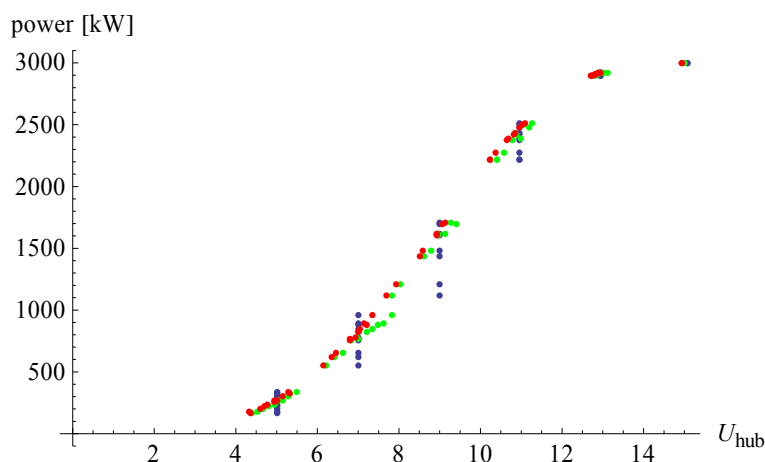

Figure 6.2 Results from Vestas' simulations. Power as function of hub height wind speed (blue), as function of U_{disk} *(red) and as function of* U_{KE} *(green).*

Figure 6.2 shows the power curves resulting from Vestas' simulations. Like the results from HAWC2Aero simulations, the scatter is clearly smaller with both the equivalent wind speed than with the wind speed at hub height. The curves obtained with the equivalent wind speeds are very similar. The main difference occurs between 7 and 8 m/s where the scatter obtained with U_{KE} increases.

7 Configuration mounted nacelle LIDAR

In all the previous sections the equivalent wind speed was derived from the wind speed taken at 11 points on a vertical line in the middle of the rotor swept area. This configuration corresponds to measurements that can be obtained with a meteorological mast or a ground based LIDAR, see figure 7.1.
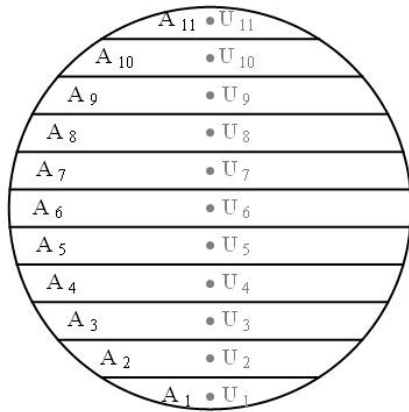

Figure 7.1 First configuration of distribution of the wind speeds over the rotor swept area with the different segments used to calculate the equivalent wind speeds.

However, simulations enable us to consider very different configurations. Thus in this section, the wind speed is given at 50 points evenly distributed on a circle with a radius 85% of the blade length, see Figure 1.a. This configuration is similar to what we could ideally obtain from a LIDAR mounted on the nacelle of the turbine and conically scanning in front of the turbine, see Figure 1.b. This configuration was inspired by the scanning pattern of a Zephir LIDAR, which measures 50 radial wind speeds per conical scanning on average.
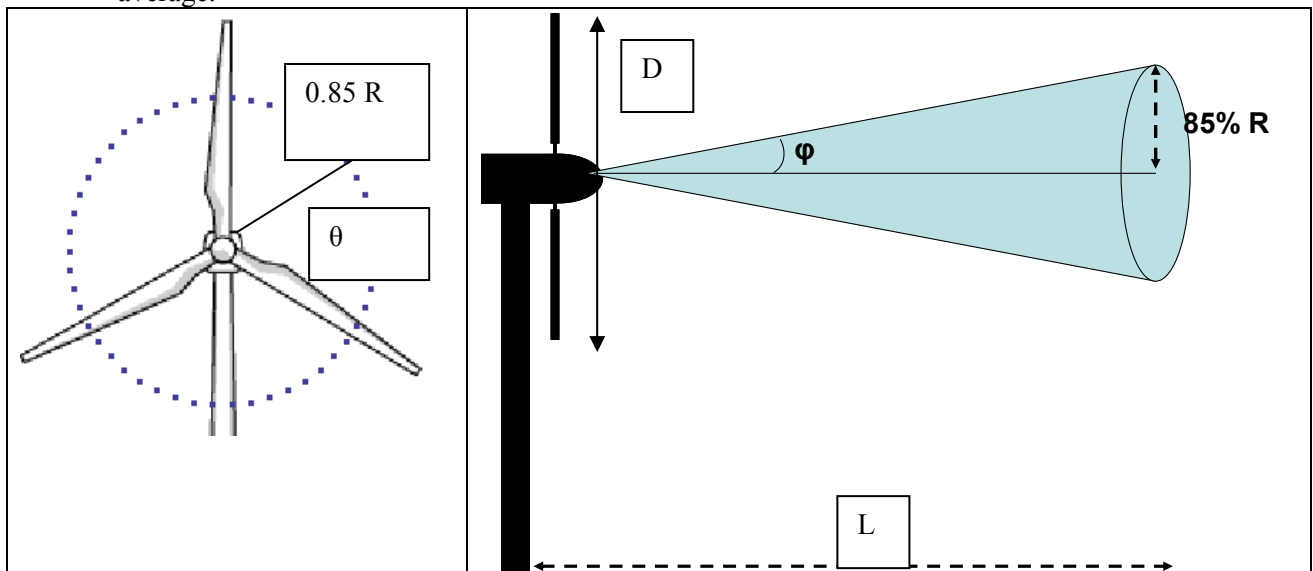
7.1 Limitations of real LIDAR measurements

A LIDAR can only measure the projection of the wind speed on the laser line-of-sight, the radial speed: $v_r(\theta) = u_x \cos(\theta)\sin(\varphi) + u_y \cos(\varphi) + u_z \sin(\theta)\sin(\varphi)$ where

$\vec{u} = (u_x, u_y, u_z)$ is the wind speed vector in the turbine related coordinate system, θ the azimuth angle, φ the LIDAR cone angle.

Note that the choice of φ depends on the radial position (r; here r=0.85R) and the distance from the turbine where we want to measure (L): $\varphi = Tan^{-1}\left(\dfrac{r}{L}\right)$. D should be chosen in order to measure the free wind speed in front of the turbine, i.e. the wind speed which is not affected by the induction effect; the IEC 61400-12-1 recommends at least 2 turbine rotor diameters. In the case simulated here, it would correspond to an angle of about 12°.

It should be noted that this is technically challenging with currently available LIDARs as they give reliable measurements only up to 150 m for cw systems (because of the resolution) and to 200m for the pulsed systems (because of the decrease of the light power (quadratically with distance) as it propagate in the air). However, this may be improved by focusing the laser bean at 200m.

In order to retrieve the full wind speed vector (three components), we need 3 radial speeds (from three positions); in practice it is therefore impossible to obtain the full wind speed vector at each measurement point.

However, for measurement in flat terrain (when the turbine is not in the wake of another turbine), it is fair to assume:

- horizontal homogeneity: $\vec{u}(x, y, z) = \vec{u}(z) = (u_x(z), u_y(z), u_z(z))$;

- $\langle u_z \rangle = 0$ (for zero tilt angle, which is assumed here).

These assumptions simplify the problem.

In case of uniform inflow, only the component along the turbine axis remains not null:
$$u_x = 0 \quad \Rightarrow \quad v_r(\theta) = u_y \cos(\varphi)$$
$$= u_{hub} \cos(\varphi)$$

The case of speed (vertical) shear, is very similar to the uniform flow; the difference is that the wind speed varies with height:
$$u_x = 0 \quad \Rightarrow \quad v_r(\theta) = u_y \cos(\varphi)$$
$$= u(z) \cos(\varphi)$$

Note: $z = H + r\sin(\theta)$, where H is the hub height, r the radial position of the measurement and θ the azimuth angle. Therefore u depends on the azimuth position (same as wind speed seen by a rotating blade), see figure 2. In those cases (uniform flow and flow with speed shear), the radial speed is proportional to u as phi is constant.
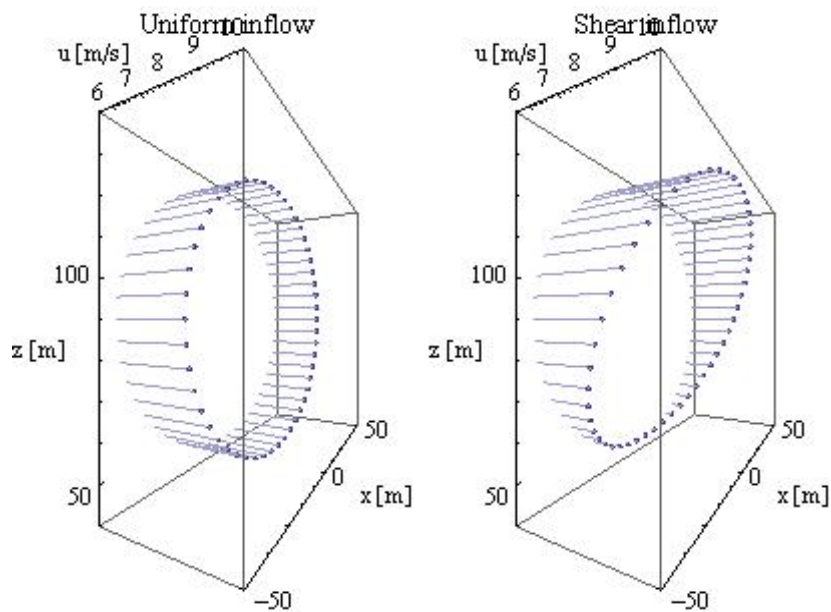
Figure 7.2 Examples of speed fields obtained with the 50 points distributed over a circle in the rotor pane (a) in case of uniform inflow, (b) in case of shear inflow following a power law (α=0.5).
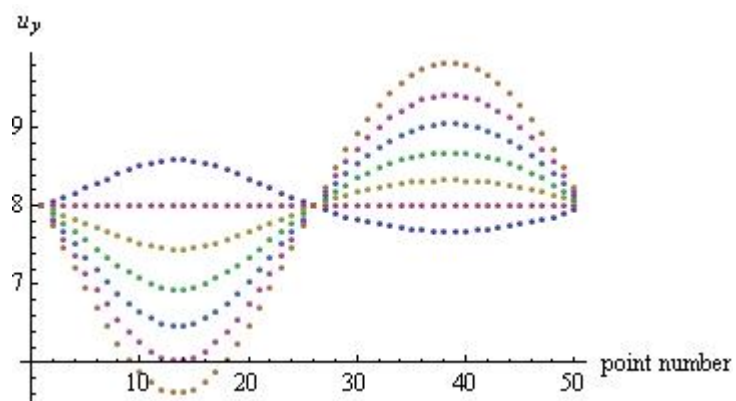

Figure 7.3 Radial speed at each of the 50 points (wind speed as function of the point number (i.e. azimuth position); number 1 ⬅➡ θ=0) for various shear exponents.

The horizontal homogeneity results in symmetry between the two half of the circle that are on each side of the vertical axis. Indeed because of the horizontal homogeneity, the wind speed is the same on both sides of the circle at one given height (positions represented by P1 and P2 in Figure 7.4). On the other hand, at those positions, the lines of sight of the LIDAR are symmetrical.
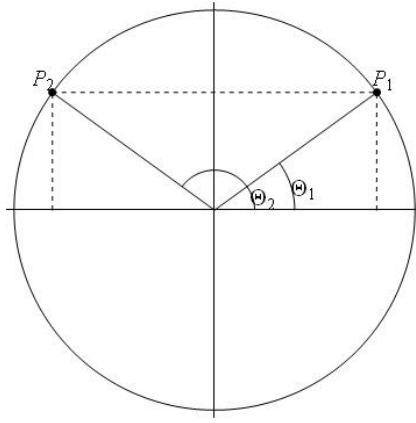
Figure 7.4 Geometry used to retrieve the horizontal speed from LIDAR measurements. P$_1$ *is defined by* θ_1 *and P2 by* $\theta_2 = \pi - \theta_1$.

Therefore, we can easily retrieve ux and uy by combining $v_r(\theta)$ and $v_r(\pi - \theta)$ (those 2 points have the same altitude: $z = H + r\sin(\theta)$), for any of the following inflow cases:

- Yaw error: $\alpha^Y = \gamma_{nacelle} - \gamma_{wind} \neq 0$;
- Direction shear: $\begin{array}{l}\alpha^S(z) = \gamma_{nacelle} - \gamma_{wind}(z)\\ \alpha^S(H) = 0\end{array}$;
- Speed shear: $u = u_y(z)$;
- Combination of all 3.

$$\begin{cases} v_r(\theta) = u(z)\sin(\alpha^Y + \alpha^S(z))\cos(\theta)\sin(\varphi) + u(z)\cos(\alpha^Y + \alpha^S(z))\cos(\varphi) \\ v_r(\pi - \theta) = -u(z)\sin(\alpha^Y + \alpha^S(z))\cos(\theta)\sin(\varphi) + u(z)\cos(\alpha^Y + \alpha^S(z))\cos(\varphi) \end{cases}$$

$$\Leftrightarrow \begin{cases} v_r(\theta) + v_r(\pi - \theta) = 2\cos(\varphi)u_y = 2\cos(\varphi)\left[u(z)\cos(\alpha^Y + \alpha^S(z))\right] \\ v_r(\theta) - v_r(\pi - \theta) = 2\cos(\theta)\sin(\varphi)u_x = 2\cos(\theta)\sin(\varphi)\left[u(z)\sin(\alpha^Y + \alpha^S(z))\right] \end{cases}$$

Note that if there is a horizontal shear of the wind speed, the symmetry between $v_r(\pi - \theta)$ and $v_r(\theta)$ is not true anymore and those formulas cannot apply. Moreover, in reality, the LIDAR measures while the laser beam is conically scanning (the beam does not stop), therefore the measurement point positions probably vary for one scan to the following. In that case, the symmetry between the positions of the measurement points is assured and the calculations suggested above are not possible. For this reason, a LIDAR system measuring the radial speeds in fixed line-of-sights would be preferable.

7.2 Power curve

With this distribution of wind speed over the rotor disc, it seems logical to divide the rotor swept area in "pizza slices" instead of segments, see Figure 7.5. As the measurements are evenly distributed, each slice area is equal to *A/50*. Then the first equivalent speed definition is the simple average of the wind speed over the profile:

$$Ueq_1 = \sum_{i=1}^{50} u_{yi} \frac{A_i}{A} = \sum_{i=1}^{50} u_{yi} \frac{1}{50}$$
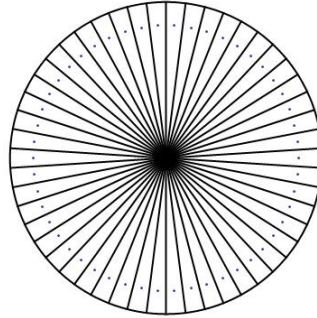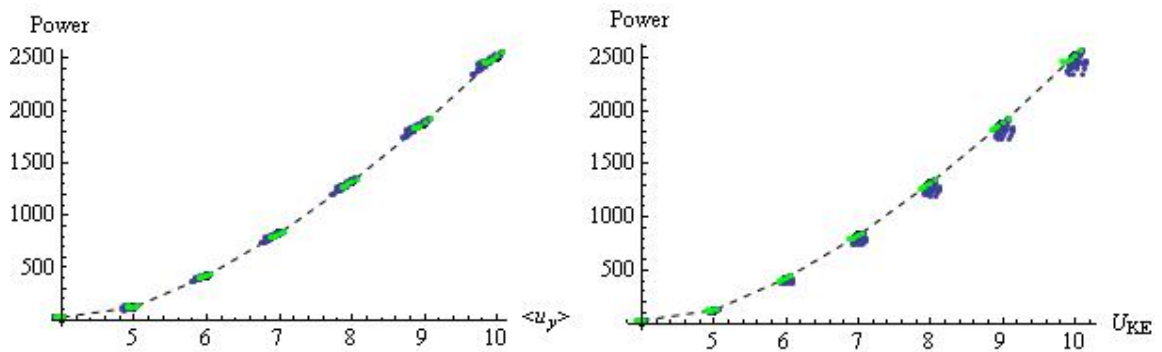

Figure 7.5 Rotor divided in 50 (equal) slices.

Figure 7.6 (Left) Power curve as function of the average of the axis wise component of the wind at the 50 points (<u$_y$>); (right) Power curve as a function of U$_{KE}$. The results showed in these plots were obtained for laminar inflow with various wind speed shear and direction shear. Black points: points obtained for uniform inflow; line: interpolation line considered as representation of the zero-shear power curve, Blue dots: power output obtained with linear direction profiles and power law speed profiles; Green dots: power output obtained with linear direction profiles and no speed profiles.
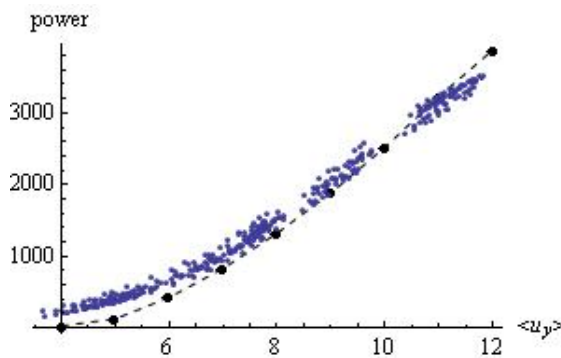

Figure 7.7 Power curve as a function of the average of the axis wise component of the wind at the 50 points(<u$_y$>). The results showed in this plot were obtained for the simulation with realistic profiles and standard turbulence intensity.

Another approach could be to use these radial wind speed data in order to retrieve the horizontal wind speed profile and use an equivalent wind speed similar to the one used with the previous configuration:
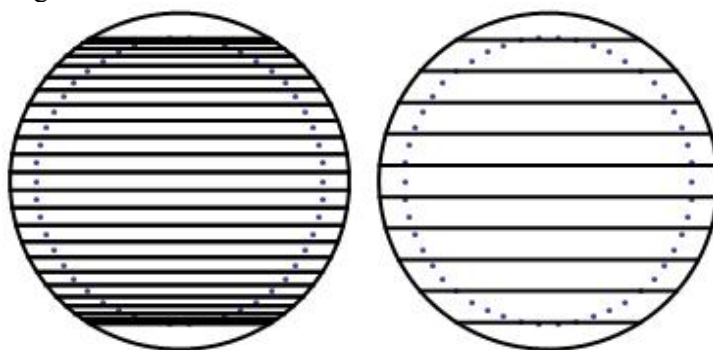

Figure 7.8 Rotor divided in horizontal segments. (a) 25 segments defined by the 25 pairs of measurement points; (b) 11 segments defined by the vertical configuration shown in Figure 7.1.

This can be done in two ways:
- consider one segment for each wind speed;
- or keep the same 11 segments as above and average the wind speeds gathered in each segment.
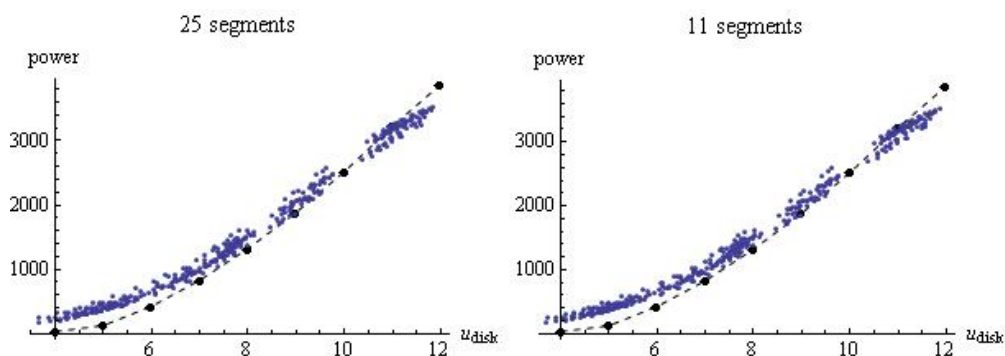

Figure 7.9 Power curve as a function of U_{disk} (left) considering the wind speeds at 25 heights (25 segments); (right) considering the mean wind speeds in 11segments. The results shown in these plots were obtained for the simulation with realistic profiles and standard turbulence intensity.

7.3 Discussion

The weighted average gave a smaller scatter than the simple average. However, this is probably again due to the assumptions inherent in the aerodynamic model.

As previously stated, the experimental application of such measurements (remote sensing from the turbine nacelle) requires measuring far enough from the turbine rotor in order to avoid the induction effect and measure the free stream speed. This requires measuring at least 2 rotor diameters upstream. However focused LIDAR are limited to 150 m. Pulsed systems showed good vertical measurement up to 200 meters, sometimes higher when there were enough aerosols. However, with pulsed system it is not possible to measure at so many points (50) fast enough. Systems currently developed for nacelle mounting work with 3 (Vindicator). As a LIDAR actually measure the speed in the line-of-sight, a system measuring in 3 directions can only give one full (3D) speed vector and does not give any information about the shear. An even number of line-of-sights symmetrically

positioned would allow obtaining 3 wind speeds (with horizontal homogeneity assumption), one at hub height, one below and one above. This raises the question of the number of wind speed measurements (to make one profile) necessary to reduce the scatter significantly. We obtained good results with 11 wind speeds, but the use of 25 wind speeds did not improve significantly. On the other hand, 3 measurement points with one above hub height give better information about the shear than measurements all below hub height.

Finally, it is important to remember that the assumption of horizontal homogeneity is still required. The configurations considered above do not enable us to easily distinguish between a yaw error and a horizontal speed shear. This system does not solve the problem of shear measurement in complex terrain.

8 General discussion

We used an aerodynamic model in order to consider the impact of shear and turbulence separately on the power performance. This enabled us to consider some very simplified but rather unrealistic situations such as laminar flow for example. However most of aerodynamic models are designed to investigate loads in uniform inflow. The case of non uniform inflow on horizontal-axis wind turbines is more delicate and very little is known about aerodynamics in shear inflow. However, within the last few years, it was recognized that large wind turbines must be subjected to non uniform inflow quite often and therefore that case should be taken into consideration in the models. For BEM models, this requires a modification of the induction calculation as a sheared inflow causes an azimuthally variation of the induction factor (whereas it is assumed to be constant over the rotor swept area in the basic BEM theory). However this can be done in several ways and so far no conclusion could be drawn about which method is the best one. This would require good agreement with more advanced models (and agreement between the advanced models) and a validation with experimental data. Therefore the use of an aerodynamic model to investigate the influence of shear on the power output presents large uncertainties and results cannot be considered as "the" expected power output in case of shear. Different results may be found with different models and experimentally.

This investigation is more of a first approach in the understanding of the influence of wind shear on the power output of a wind turbine. All results presented here are restricted to the assumptions made in HAWC2Aero (and to the assumption of horizontal homogeneity of the inflow). However, it is worth to note that similar results were obtained with Vestas' model.

Both speed and direction shear create fluctuations in the aerodynamics of a wind turbine and this has an opposite impact on the power output. The speed shear (power law profiles) results in decreasing the power output with increasing shear coefficient. However one has to be careful when having this conclusion because the first difference between a shear flow and a uniform inflow is the kinetic energy flux it generates. Secondly, the simulations showed that two profiles with the same kinetic energy flux do not necessarily generate the same power output from the turbine. Moreover, whereas power law profiles resulted in moderate variations of the power, the simulations carried out with profiles different from the power law model (but still realistic) resulted in larger variation of the power.

The variation in power output resulted in an increase in scatter of the power curve if only the wind speed at hub height was considered (as required in the current standard). This scatter due to the wind speed shear could be decreased by using an equivalent wind speed accounting for the shear. Such an equivalent wind speed can be defined in several ways. We investigated two definitions: an average of the wind speed over the rotor swept area and an approximation of the kinetic energy flux taking the wind shear into account. However, due to the uncertainties in the modeling, the simulations did not enable us to conclude about the best definition. The weighted average resulted in a smaller scatter but this almost certainly due to normalization of the torque coefficient using such an average wind speed in HAWC2Aero. The aerodynamic simulations then do not appear as an ideal tool to find the best equivalent speed definition. It would require a more advanced model with fewer assumptions in the response of the turbine to a non uniform inflow.

Furthermore, according to the simulations, a small positive direction gradient results in a slight increase of the power output whereas a larger positive direction gradient decreases the relative power output and a negative gradient always results in a decrease of the power output. In situ measurements analysis generally shows rather small (positive) gradient and very seldom anticlockwise direction shear in the Northern hemisphere. Therefore, the direction shear is expected to have a smaller impact on the turbine power output than the

speed shear. A simple correction (with a cosine function) in the equivalent wind speed definition resulted in a reduction of the scatter in the power curve. However, it cannot be the best correction as we saw that the behavior of the power output as function of the direction gradient was not symmetrical around 0. Moreover, only linear direction gradients were used in this investigation. Real direction profiles may deviate from this simple model.

The effect of turbulence on the power output is different from the effect of shear. The main effect that is observed in the power curve is the result from the use of 10 minutes averaged data. The shape of the mean power curve varies with the turbulence intensity (especially around rated wind speed) and a power curve obtained with various turbulence intensities would therefore results in a large scatter. Including the turbulence intensity in the kinetic energy flux calculation then gives a better approximation of the power available in the wind. However using an equivalent wind speed based on this approximation of the kinetic energy flux cannot reduce the scatter as the turbine cannot extract the power from the wind fluctuations. Normalising the power to a given turbulence intensity appears as the best solution so far. In spite of this, it was shown that the equivalent wind speed method was still interesting when shear and turbulence were combined.

It is difficult to conclude on which parameter between speed shear, direction shear and turbulence had the largest effect on the power output. First because it depends on the range of magnitude of each parameter, e.g. it depends on the site and the season; secondly because of the high uncertainty in the model.

Finally, if we want to apply such a method experimentally, several ways of obtaining the shear information are possible. Two configurations were considered here:
- o Wind speed given at 11 points vertically aligned (similar to a meteorological mast and ground based remote sensing instrument);
- o Wind speed given at 50 points distributed over a circle with a radius of 0.85R (similar to a LIDAR mounted on the nacelle).

These two configurations gave very similar results in power curve scatter. It is important to remember that both ground based and nacelle mounted LIDAR require us to assume a horizontal homogeneity of the flow and therefore cannot be directly used in complex terrain. One of the main advantages of the measurements obtained from an instrument based on the nacelle is that it increases the acceptable sector to all direction where the turbine is not in the wake of an obstacle (and the LIDAR's laser is not blocked by any obstacle).

9 Conclusions

Aerodynamic simulations were used to investigate the influence of speed shear, direction shear and turbulence separately on the power output of a large wind turbine. The results showed that an inflow with power law wind speed profiles moderately decreases the power output compared to a uniform inflow; larger variations of the power can be obtained with different profiles. Secondly, the direction shear had a smaller impact on the power output than the speed shear, but a small clockwise direction gradient could slightly increase the power output. The use of an equivalent wind speed taking the shear into account decreased the scatter due to shear in the power curve and this could still be seen in the case of high turbulence intensity. However due to the ambiguity concerning calculation of the induced velocities in non-uniform flow, such a model presents large uncertainties in the power output for sheared inflow and the results of this work are limited to the model used. This investigation could be completed with simulations of similar cases with a more advanced model such as a CFD model and with comparisons to measurements.

References

Antoniou I., 2009. *Wind shear and uncertainties in power curve measurement and wind resources*, WindPower 2009.

Albers A., 2007. *Influence of meteorological variables on measured wind turbine power curve*, EWEC 2007

Bak K., 2006. *Research in aeroelasticity EFP 2006*, Risø-R-1611

Christensen CJ et al., 1988. *Accuracy of Power Curve Measurements*, Risø-M-2632

IEC standard 61400-12-1

Elliott D.L., Cadogan J.B., 1990. *Effects of wind shear and turbulence on wind turbine power curve*, EWEC 1990

Gottschall J., *Modelling the variability of complex systems by means of Langevin processes*, PhD thesis. http://oops.uni-oldenburg.de/volltexte/2009/874/pdf/gotmod09.pdf

Kaiser K., 2003. *Turbulence Correction for Power Curves*, EWEC 2003

Larsen T.J., 2006. *Influence of blade pitch loads by large blade deflections and pitch actuator dynamics using the new aeroelastic code HAWC2*, EWEC 2006

Larsen T.J., 2007. *HAWC2, the user's manual*, Risø-R-1597(ver.3-1)

Larsen T.J., 2008. *HAWC2Aero, the user's manual* , Risø-R-1631(ver.1-0)

Madsen H.A., 2003. *Yaw aerodynamics analyzed with three codes in comparison with experiment*, AIAA-2003-0519.

Madsen H.A., 2008. *Short comings in state of the art engineering aerodynamic and aeroelastic models by comparison to advanced models*, Risø-I-2522.

Mann J., 1998. *Wind field simulation*, Prob. Enng. Mech. **13**-4: 269-282

Manwell J.F., McGowan J.G., Rogers A.L. 2002, *Wind energy explained: Theory, Design and Application*, Wiley.

Moore K, 2006. *Observed rotor-plane wind profiles derived from sodar measurements: potential impact on turbine power performance*, WindPower 2006.

Pedersen T.F., 2004. *On Wind Turbine Power Performance Measurements at Inclined Airflow*, Wind Energy **7**: 163-176.

Sumner J., Masson C., 2006. *Influence of Atmospheric Stability on Wind Turbine power Performance Curves*, Journal of Solar Energy Engineering, 128:531-538.

Swalwell K.E. et al. 2008. *Diurnal wind characteristics and WTG loading*, EWEC2008.

Van deb Berg G.P., 2008. *Wind Turbine Power and Sound in Relation to Atmospheric stability*, Wind Energy, 11:151-169.

Wagner R., 2009. Antoniou I., Pedersen S.M., Courtney M., Jørgensen H.E, 2009 *The influence of the wind speed profile on wind turbine performance measurements*, Wind Energy, 12:348-362.

Walter K., 2007. *Wind power systems in the stable nocturnal boundary layer* (Thesis)

Walter K. et al., 2009. *Speed and Direction shear in the Stable Nocturnal Boundary Layer*, Journal of Solar Energy Engineering, **130**

Annex A:
## Simplified speed triangles for shear inflow

1 No Shear (reference case)
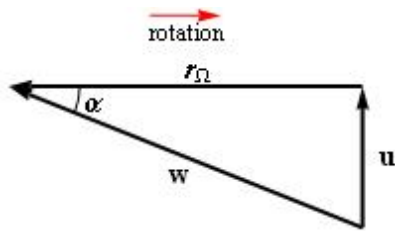
The wind speed seen by the blade (u), and the therefore the angle of attack (alpha) and the relative speed (w) are the same at any azimuthal position.

Note that on that figure, alpha is the angle between the rotor plane and the relative speed (**w**) which is actually the sum of the angle of attack, twist angle and pitch angle. However, the twist angle depends on the position on the blade and here we consider always the same one. Moreover, for speeds below rated, the pitch angle is set to zero by the controller. Therefore, the variations of alpha represent the true variation of the angle of attack.

2 Speed shear
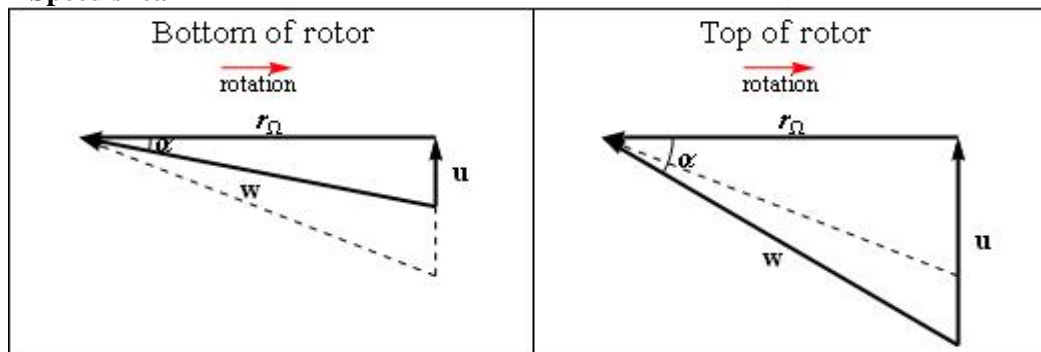
In this figure a linear profile is assumed (the argument would be the same for a power law profile). For comparison purpose the speed triangle at hub height is shown with dashed arrows.
Below hub height, the wind speed is smaller than hub height speed. Consequently the relative speed (w) and the angle of attack (alpha) are smaller than those at hub height. Above hub height, the wind speed is higher than hub height speed. Consequently the relative speed (w) and the angle of attack (alpha) are higher than those at hub height. This complies with the variations shown in Figure 3.4 (although the model accounted for induction).

3 Clockwise direction shear (veer)
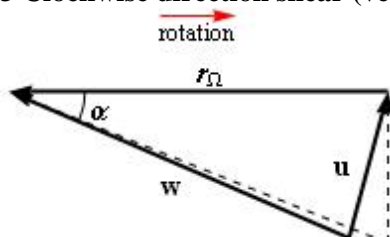
In the case of clockwise direction shear, the magnitude of the wind speed is the same at all heights whereas the direction changes. For a linear variation of the wind direction with

height (and no yaw error at hub height), the speed triangles are the same at the top and the bottom of the rotor (see figure above). The relative speed (w) is smaller whereas the angle of attack is larger than those at hub height.

4 Anticlockwise direction shear
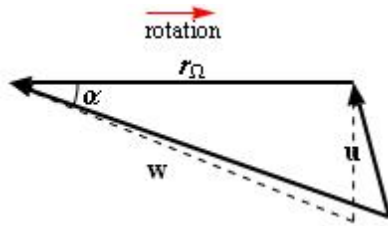
This situation is the opposite of the previous one. The relative speed (w) is larger whereas the angle of attack is smaller than those at hub height.

For those specific two cases (linear direction shear with no yaw error and exactly the same amplitude):

$$\left|\alpha^+ - \alpha^0\right| \leq \left|\alpha^- - \alpha^0\right|$$

$$\left|w^+ - w^0\right| \leq \left|w^- - w^0\right| \text{ but very small dif}$$

Note that all these consideration may fall due to the induction directly modifying the speed triangles. Moreover the rotation of the wake may cancel the symmetries assumed in the situations above which would result in non sinusoidal variation of the relative speed and the angle of attack with azimuth.

5 Yaw error
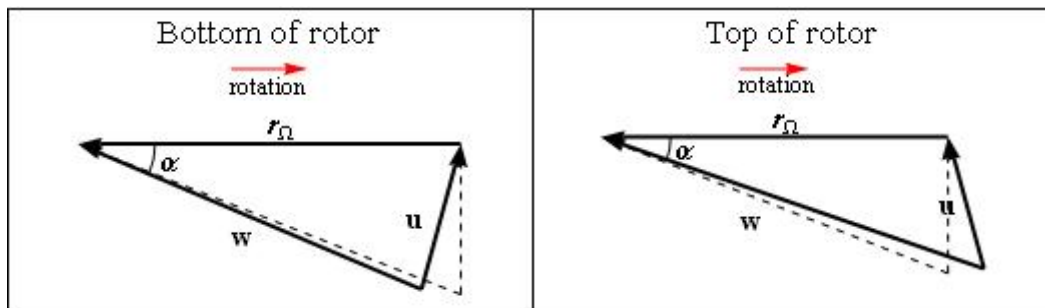
A yaw error situation is different from a direction shear as the inflow angle with the rotor is the same all over the rotor swept area. This results in different speed triangles at the top and the bottom of the rotor.

Annex B:
Selection of wind profiles to be used as input for wind turbine power simulation

Step 1: Binning of the 10 min average profiles measured at Høvsøre in 2006 according to the wind speed at hub height for the range of 4 m/s to 16m/s in bins large of 2 m/s; which gives 6 bins: 5m/s, 7m/s, 9m/s, 11 m/s, 13 m/s, 15 m/s.

Step 2: In each wind speed bin, the profiles have been grouped according to their shape (shear) and then averaged. (This gives between 100 and 200 different shapes for each wind speed bin.)

Step 3: In each wind speed bin, 10 of the previous "shapes" were selected in order to get 10 different kinetic energy flux** after normalization*.

*Profile normalization:
In order to observe the influence of the wind shear (only the shear and not the wind speed at hub height, in each wind speed bin, the 10 selected profiles were normalized so they have the same wind speed at hub height (the mean wind speed of the bin: 5m/s, 7m/s, 9m/s,…).

$$U^N = U \times \frac{U_h^N}{U_h}$$

U: wind speed at any height but hub height,

U_h: wind speed at hub height,

U^N: normalized U,

U_h^N: normalized U_h.

In order to keep the same turbulence intensity as measured, the standard deviation has to be normalized as well.

$$\sigma^N = \sigma \times \frac{U_h^N}{U_h}$$
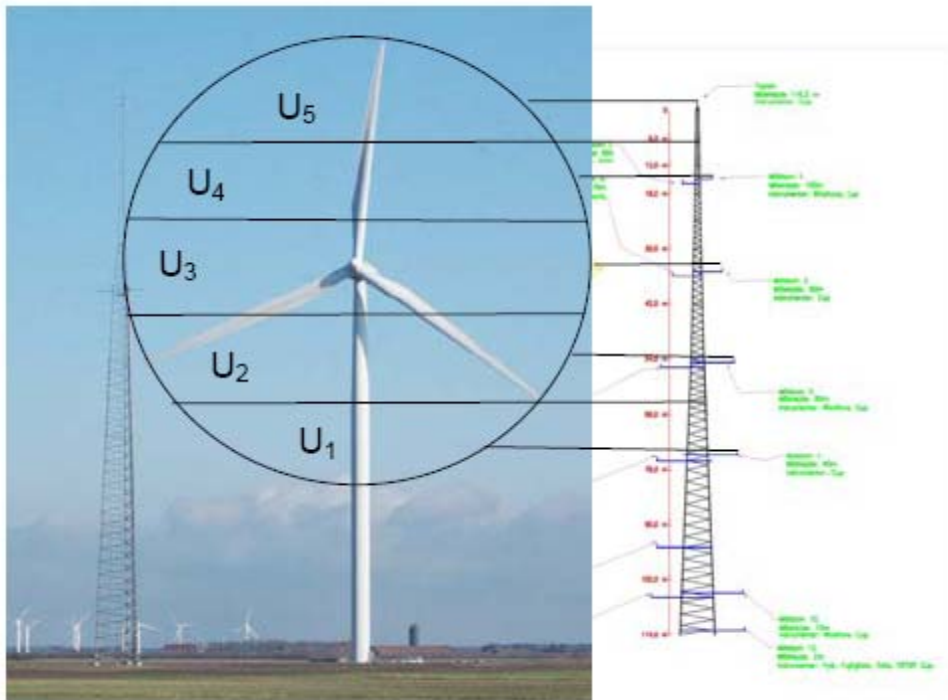
σ: wind speed standard deviation,

σ^N: normalized σ.

Thus $\frac{\sigma^N}{U^N} = \frac{\sigma}{U}$.

** Evaluation of the kinetic energy flux taking the shear into account:
The rotor disc is divided into 5 horizontal areas A_i (see figure below), within each of which the wind speed is assumed uniform and equal to 10 min average measured by the cup at the corresponding height U_i. The kinetic energy flux through the whole rotor disc can then be approximated by the sum of the KEflux of each area:

$$KEflux \simeq \sum_{i=1}^{5} U_i^3 \times A_i$$

Risø-R-1722(EN)

Note: the normalized mean wind speed and standard deviation profiles are compared to the profiles from the international standard IEC 61400-1.

For any further information: rozenn.wagner@risoe.dk.
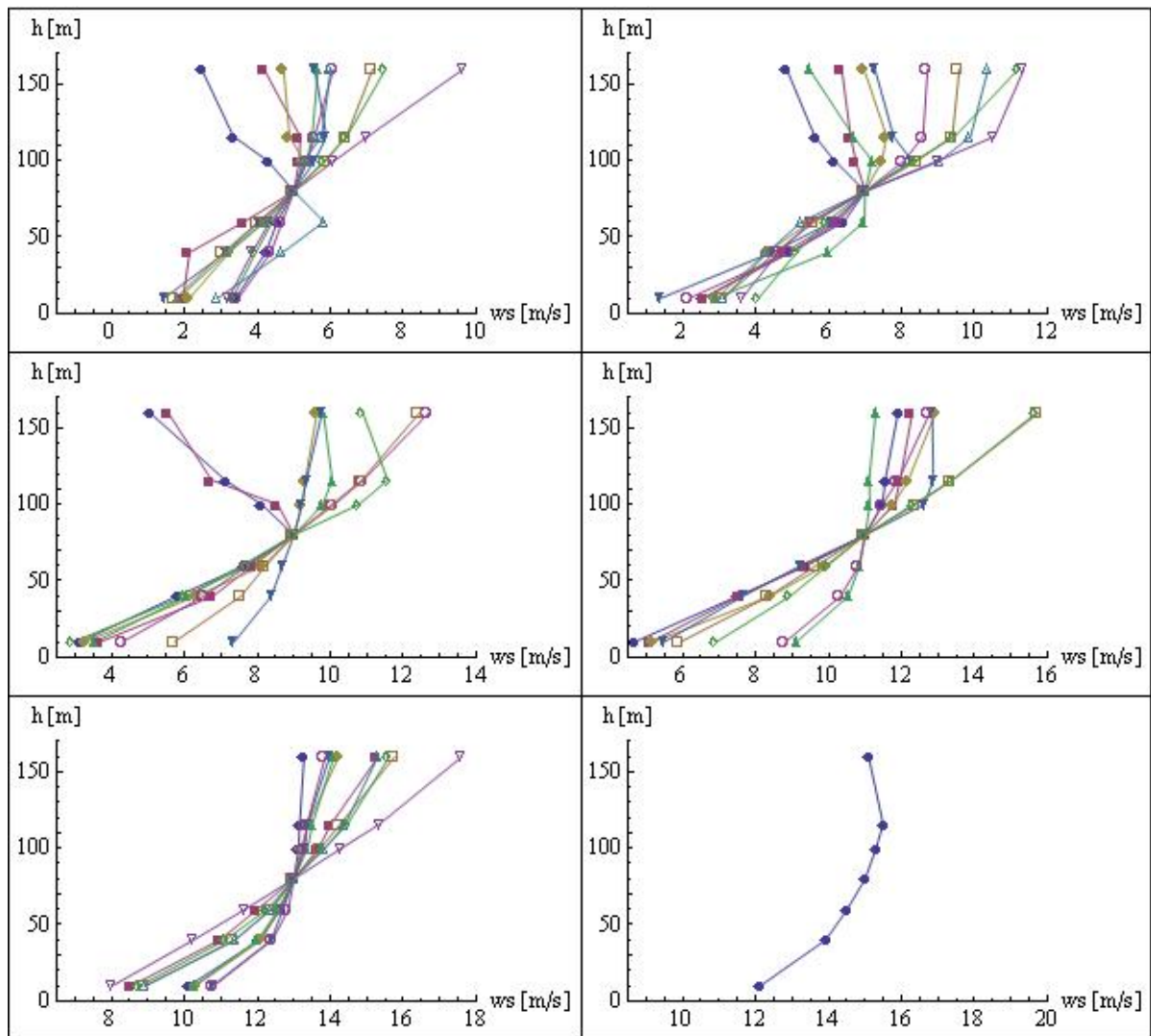
Risø DTU is the National Laboratory for Sustainable Energy. Our research focuses on development of energy technologies and systems with minimal effect on climate, and contributes to innovation, education and policy. Risø has large experimental facilities and interdisciplinary research environments, and includes the national centre for nuclear technologies.